ERS-2 Wind Scatterometer
Cyclic Report

From 21st February 2005 to 28th March 2005
Cycle 103

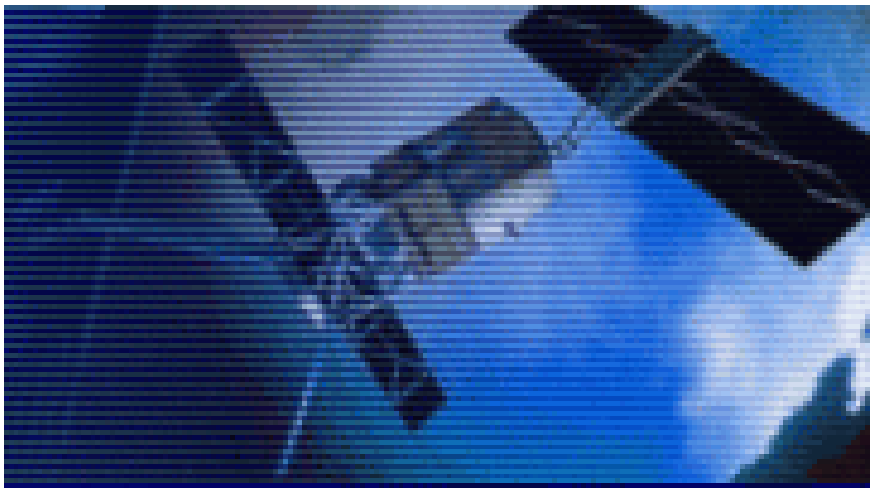

Prepared by: PCS Team
Inputs from: H. Hersbach (ECMWF)

Issue: 1.0
Reference ERSE-SPPA-EOPG-TN-05-0004
Date of issue: 12th May 2005
Status: Approved
Document type: Technical Note
Approved by: P. Lecomte

Table of Content

1

Introduction and Summary

The document includes a summary of the daily quality control made within the PCS and various sections describing the results of the investigations and studies of "open-problems" related to the Scatterometer. In each section results are shown from the beginning of the mission in order to see the evolution and to outline possible "seasonal" effects. An explanation for the major events which have impacted the performance since launch is given, and comments about the recent events which occurred during the last cycle are included. This report covers the period from 21st February 2005 to 28th March 2005 (cycle 103) and includes the results of the monitoring activity performed by ESRIN and ECMWF.

• This document is available on line: http://earth.esa.int/pcs/ers/scatt/reports/pcs_cyclic/

Mission events

• The ERS-2 satellite was piloted in ZGM throughout the cycle 103.
• During cycle 103 the ESACA processor worked nominally without faults.
• The AMI instrument was unavailable on February 26th (01.20 a.m. – 12.37 a.m.) and on March 11th (02.43 p.m. – 05.41 p.m.) due to an emergency switch-down.
• For the entire period in cycle 103, ERS-2 Scatterometer data was used in the 4D-Var data assimilation system at ECMWF.
• News on ERS mission is available on line: http://earth.esa.int/ers/new_ers_news.html

Yaw performance

• The result of the yaw monitoring for cycle 103 is a yaw error angle within the expected nominal range (+/- 2 degrees) with an average level around 0 deg. for most of the orbit. Since mid March 2005 there was an improvement in the yaw performances. This is mainly due to the geometry of the Earths orbit that decreases the negative impact of the Sun within the field of view of the Earth sensor at the Eclipse to Sunlight transition (see previous report for details).
In the case of strong degraded yaw, in the delivered products, the combined kp and yaw-error flag is set, allowing the users to reject the low quality measurements.

Calibration performance

• Calibration data from Transponder are regularly acquired and archived for re-processing. The TOSCA (Tool for Scatterometer CAlibration) project is ongoing. The oSAT of the tool has been performed as scheduled at the end of April 2005. Calibration results will be provided in the next reports.
• Due to the regional mission scenario the calibration performances over the Brazilian rain forest are not available because that area is not covered by the ESA ground station. The chance to install a new station to cover the calibration site is under investigation as well as the possibility to use stable ice area in Greenland to monitor the instrument calibration.
• The Ocean Calibration monitoring is performed by ECMWF. Sigma bias levels are about 0.2 dB more negative compared to those during cycle 102. Inter-node and inter-beam dependencies are still small, although the levels of the descending mid and aft beam are about 0.2 dB higher than that for other beams. Average bias level is around -0.45 dB, which is 0.05 dB less negative than for nominal data in 2000.

Instrument performance

• During the cycle 103 the mean transmitted power evolution was very stable. The mean decrease has been very small (0.03 dB per cycle), it was 0.14 dB for cycle 102. To confirm or not that stabilization a long time period of observations is needed. A final conclusion will be available in the next reports.
• The evolution of the noise power during the cycle 103 was stable. The daily average noise power for the Fore and Aft beam was around 1.7 ADC (I) and around 1.6 ADC (Q) respectively. For the Mid beam the noise is not measurable.
• During the cycle 103 the Doppler compensation evolution was stable. The CoG of the compensated signal was around 0 Hz for the Fore and Aft antenna and around 200 Hz for the Mid antenna. The standard deviation of the CoG was around 1500 Hz for the Fore and Aft antenna and around 2700 Hz for the Mid antenna. Those values are as for cycle 102. The small variations on the CoG evolution on 8th and 11th March 2005 are due to orbital manoeuvres.

Product performance

During cycle 103 data was received at ECMWF between 21:04 UTC 21 February 2005 and 20:58 UTC 28 March 2005. No data was received for the 6-hourly data batch of 06 UTC 26 February 2005 (AMI instrument anomaly), 00 UTC 2 March 2005 and 00 UTC 3 March 2005.

Compared to cycle 102, the comparison of the UWI wind speed with ECMWF first-guess (FG) fields showed a similar relative standard deviation (1.56 m/s to 1.55 m/s). The relative bias has become more negative (from -0.65 m/s to -0.72 m/s). For winds based on CMOD5 the negative bias has grown as well (from -0.08 m/s to -0.18 m/s). Both relative bias levels and standard deviation are better to those for 2000.

The PCS geophysical monitoring reports a slight degradation of the winds performances. The wind speed bias (UWI vs 18 or 24 hour forecast) was roughly 0.7 m/s (it was 0.6 m/s for cycle 102) and the speed bias standard deviation was around 1.8 m/s (it was 1.6 m/s for cycle 102). Those values are very similar to the ones computed by ECMWF. Since mid March 2005 onwards the numbers of valid nodes had increased. The reason was an improvement of the Yaw performances that had reduced the number of flagged nodes.

2 Calibration Performances

The calibration performances are estimated using three types of target: a man made target (the transponder) and two natural targets (the rain forest and the ocean). This approach allow us to design the correct calibration using a punctual but accurate information from transponders and an extended but noisy information from rain forest and ocean for which the main component of the variance comes from the geophysical evolution of the natural target and from the backscattering models used. These aspects are in the calibration performance monitoring philosophy. The major goals of the calibration monitoring activities are the achievement of a “flat” antenna pattern profile and the assurance of a stable absolute calibration level.

2.1 Gain Constant over transponder

One gain constant is computed per transponder per beam from the actual and simulated two-dimensional echo power, which is given as a function of the orbit time and range time. This parameter clearly indicates the difference between “real instrument” and the mathematic model. In order to acquire data over the transponder the Scatterometer must be set in an appropriate operational mode defined as “Calibration Mode”. Since January 2001 with the operations in Zero Gyro Mode (ZGM) the satellite attitude is not stable as it was in the nominal Yaw Steering Mode (YSM). In particular there is a non-predictable variation of the yaw error angle along the orbit. For that reason the gain constant data computed by the CALPROC processor, that assumes a stable orbit, are meaningless and a new calibration processor is under development. In the mean time, data from the Transponder are still acquired and archived for future re-processing. The reprocessed gain constants will be provided in this section when available. For the gain constant computed during the nominal YSM please refer to the Scatterometer cyclic report cycle 60.

2.2 Ocean Calibration

The average sigma0 bias levels (compared to simulated sigma0's based on ECMWF model FG winds) stratified with respect to antenna beam, ascending or descending track and as function of incidence angle (i.e. across-node number) is displayed in Figure 1.

Sigma bias levels are about 0.2 dB more negative compared to those during cycle 102. Inter-node and inter-beam dependencies are still small, although the levels of the descending mid and aft beam are about 0.2 dB higher than that for other beams. Average bias level is around -0.45 dB, which is 0.05 dB less negative than for nominal data in 2000.

The data volume of descending and ascending tracks is similar.

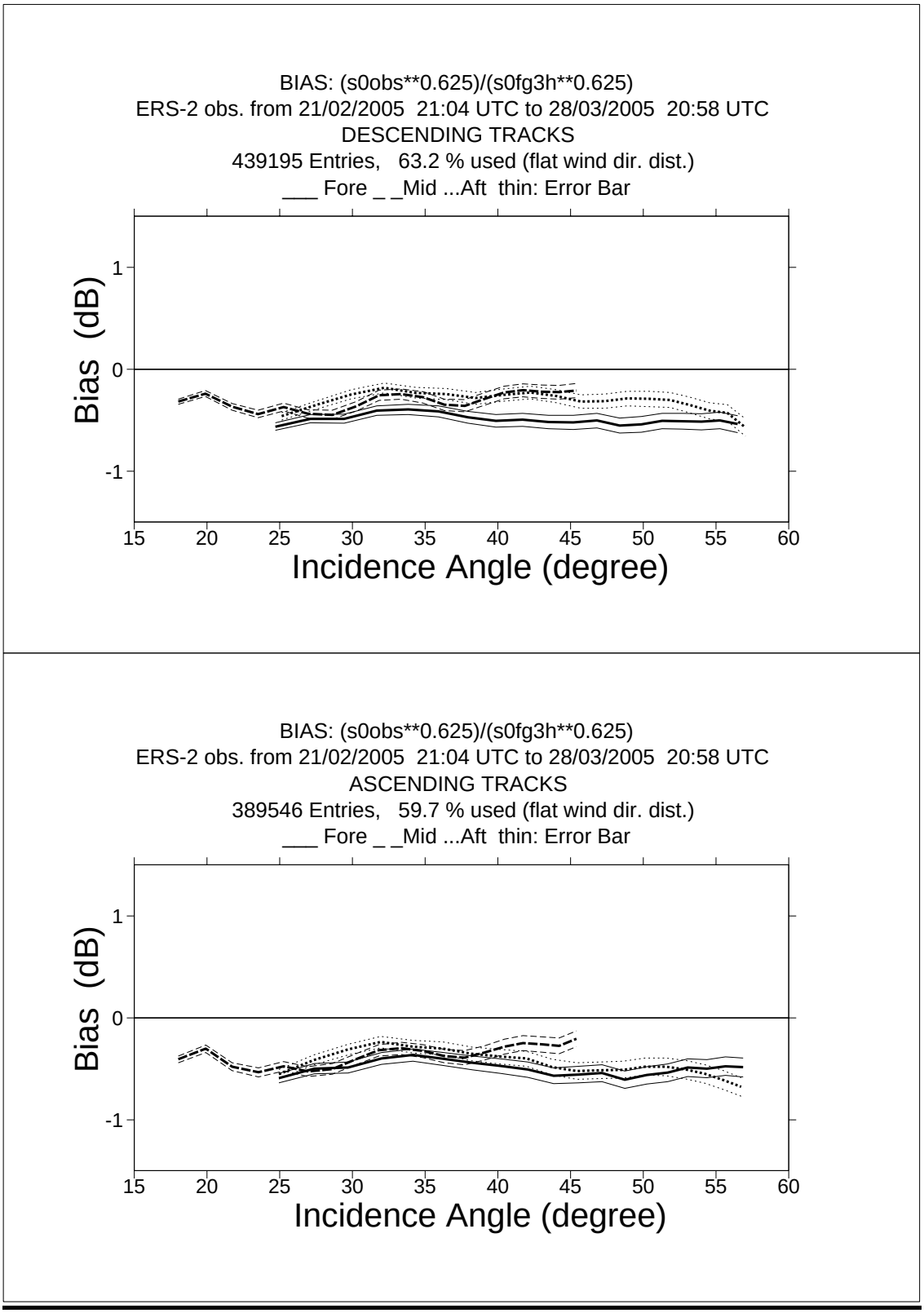

FIGURE 1 ERS-2 Scatterometer Ocean Calibration cycle 103. Ratio of <sigma_0^0.625>/<CMOD4(First Guess)^0.625> converted in dB for the fore beam (solid line), mid beam (dashed line) an aft beam (dotted line), as a function of incidence angle for descending and ascending tracks. The thin lines indicate the error bars on the estimated mean. First-guess winds are based on the in time closest (+3h, +6h, +9h, or +12h) T511 forecast field, and are bilinearly interpolated in space.

2.3 Gamma-nought over the Brazilian rain forest

Although the transponders give accurate measurements of the antenna attenuation at particular points of the antenna pattern, they are not adequate for fine tuning across all incidence angles, as there are simply not enough samples. The tropical rain forest in South America has been used as a reference distributed target. The target at the working frequency (C-band) of ERS-2 Scatterometer acts as a very rough surface, and the transmitted signal is equally scattered in all directions (the target is assumed to follow the isotropic approximation). Consequently, for the angle of incidence used by ERS-2 Scatterometer, the normalized backscattering coefficient (sigma nought) will depend solely on the surface effectively seen by the instrument:

$$S^0 = S \bullet \cos\theta$$

With this hypothesis it is possible to define the following formula:

$$\gamma^0 = \frac{\sigma^0}{\cos\theta}$$

Using the above equation, the gamma nought backscattering coefficient over the rain forest is independent of the incident angle, allowing the measurements from each of the three beams to be compared. The test area used by the PCS is located between 2.5 degrees North and 5.0 degrees south in latitude and 60.5 degrees West and 70.0 degrees West in longitude. That area is actually not covered by the Regional mission scenario (since cycle 86 onwards) and therefore the calibration monitoring activity over the Brazilian rain forest is suspended because no data are available. The chance to continue the monitoring activity with a new receiving station covering the Brazilian rain forest is under investigation. The following paragraphs will report on the results when data will be available.

2.4 Antenna pattern: Gamma-nought as a function of elevation angle

Due to the regional mission scenario data over the Brazilian rain forest are not available. For that reason the antenna patterns in function of the elevation angle have not been computed.

2.5 Antenna pattern: Gamma-nought as a function of incidence angle

Due to the regional mission scenario data over the Brazilian rain forest are not available. For that reason the antenna patterns in function of the incidence angle have not been computed.

2.6 Gamma nought histograms and peak position evolution

As the gamma nought is independent from the incidence angle, the histogram of gamma nought over the rain forest is characterized by a sharp peak. The time-series of the peak position gives some information on the stability of the calibration. This parameter is computed by fitting the histogram with a normal distribution added to a second order polynomial:

$$F(x) = A_0 \cdot \exp\left(-\frac{z^2}{2}\right) + A_3 + A_4 \cdot x + A_5 \cdot x^2$$

where: $z = \frac{x - A_1}{A_2}$

The parameters are computed using a non linear least square method called “gradient expansion”. The position of the peak is given by the maximum of the function F(x). The histograms are computed weekly (from Monday to Sunday) for each antenna individually “Fore”, “Mid” and “Aft” and for ascending and descending passes with a bin size of 0.02 dB. Due to the regional mission scenario data over the Brazilian rain forest are not available and the histograms have not been computed. For the time series since the beginning of the mission please refer to the Scatterometer cyclic report cycle 86.

2.7 Gamma nought image of the reference area

Due to the regional mission scenario data over the Brazilian rain forest are not available and the histograms have not been computed.

2.8 Sigma nought evolution

Due to the regional mission scenario data over the Brazilian rain forest are not available. For that reason none update has been done to the sigma nought evolution time series. For the time series since the beginning of the mission until June 2003 please refer to the Scatterometer cyclic report cycle 86.

2.9 Antenna temperature evolution over the Rain Forest

Due to the regional mission scenario data over the Brazilian rain forest are not available.
For the time series since the beginning of the mission please refer to the Scatterometer cyclic report cycle 86.

3

Instrument performance

The instrument status is checked by monitoring the following parameters:

• Centre of Gravity (CoG) and standard deviation of the received signal spectrum after the on-ground Doppler Compensation filter. This parameter is useful for the monitoring of the orbit stability, the performances of the Doppler compensation filter, the behavior of the yaw steering mode and the performances of the devices in charge for the satellite attitude (e.g. gyroscopes, Earth sensor, Sun sensor).

• Noise power I and Q channel.

• Internal calibration pulse power.

The latter is an important parameter to monitor the transmitter and receiver chain, the evolution of pulse generator, the High Power Amplifier (HPA), the Traveling Wave Tube (TWT) and the receiver. These parameters are extracted daily from the UWI products and averaged. The evolution of each parameter is characterized by a least square line fit. The coefficients of the line fit are printed in each plot.

3.1 Centre of gravity and standard deviation of received power spectrum

The Figure 2 shows the evolution of the two parameters for each beam since the beginning of the ERS-2 mission and Figure 3 shows the same evolution only for the cycle103.

The tendency during the nominal Yaw Steering Mode (YSM) period (beginning of the mission since the operation with the Mono Gyro (MGM) Attitude On-board Control System (AOCS) configuration on 7th February 2000) is a small and regular increase of the Centre of gravity (CoG) of received spectrum for the three antennae. During the YSM, two small changes can be detected in the CoG evolution. The first change is from 24th, January 1996 to 14th, March 1996, the second one is from 14th February 1997 to 22nd April 1997. The reason was a change in the pointing subsystem (DES reconfiguration) side B instead of side A after a depointing anomaly (see table 1 for the list of the all AOCS depointing anomaly occurred during the ERS-2 mission). During these periods side B was switched on. It is important to note that during the first time a clear difference in the CoG of the received spectrum is present only for the Fore antenna (an increase of roughly 100 Hz) while during the second time the change has affected all the three antennae (roughly an increase of 200 Hz, 50 Hz and 50 Hz for the fore, mid and aft antenna respectively).

At the beginning of 2000 the nominal 3-gyroes AOCS configuration (plus one Digital Earth Sensor -DES, and one Digital Sun Sensor -DSS and backups) was no more considered safe because 3 of the six gyros on-board were out of order or very noisy. For that reason the MGM was implemented as default piloting mode. The MGM configuration was designed to pilot the ERS-2 using only one gyro plus the DES and the DSS modules. Scope of ZGM configuration was to extend the satellite lifetime by using the available gyros one at the time.

With the MGM, an increase of roughly 200 Hz was observed at the end of the qualification period. After the AOCS commissioning phase this parameter further evolved within the nominal range with a negligible impact on the data quality.

In MGM configuration, the gyro 5 was used until 7th October 2000 when it failed. From 10th October 2000 to 24th October 2000 the gyro 6 was used. This explains the decrease of roughly 100Hz in the CoG of the received spectrum. From 25th October 2000 to 17th January 2001 the gyro 1 was used to pilot the ERS-2 satellite. On 17th January 2001 the AOCS was upgraded. The new configuration allows piloting the satellite without gyroscopes. Unfortunately a failure of the Digital Earth Sensor (DES A-side) caused ERS-2 to enter in Safe-Mode on the same day. On 25th January 2001 gyro #1 also failed.

Satellite attitude was recovered on 5th February 2001 with a coarse attitude control mode (EBM). During the period of safe mode the spacecraft had drifted out of the nominal dead band by some 30 Km. The nominal orbit was reached on 6th February 2001.
The EBM mode had a strong negative impact on the Scatterometer data quality and the dissemination of data products to end users was discontinued.

After that a series of AOCS upgrades has been implemented in order to improve the satellite attitude: on 30th March 2001 the Yaw steering law was re-introduced into the piloting function and on 7th June 2001 the Zero Gyro Mode (ZGM) has been implemented as nominal piloting mode. In ZGM the satellite attitude had an improvement in particular for the pitch and yaw error angle. This explains the reduction of the fluctuation in the received signal.

The CoG returns within its nominal value in February 2003 when the new ERS Scatterometer ground processor (ESACA) was put in operation (only for validation purposes) in Kiruna station. ESACA is able to compensate for errors in satellite attitude and to produce calibrated sigma noughts.

The evolution of the standard deviation of the CoG of the received spectrum was stable during the YSM phase. Small peaks are related with the events listed in Table 2. In MGM the evolution was within the nominal range while for the initial phase of the ZGM the performance was strong degraded. This because the on-ground Doppler filters was not able to compensate for the satellite degraded attitude. The introduction of the ESACA processor in February 2003 cured the problem.

TABLE 1 ERS-2 Scatterometer AOCS depointing anomaly list

Start of the anomaly			**End of the anomaly**			**Remarks**
24th January	1996	9:10 a.m.	26thJanuary	1996	6:53 p.m.	AOCS depointing anomaly
14th February	1997	1:25 a.m.	15thFebruary	1997	3:44 p.m.	AOCS depointing anomaly
3rd June	1998	2:43 p.m.	6th June	1998	12:47 a.m.	AOCS depointing anomaly
1st September	1999	8:50 a.m.	2nd September	1999	1:28 a.m.	
7th October	2000	4:38 p.m.	10th October	2000	4:49 p.m	depointing anomaly gyro 5 failure
24th October	2000	4:05 p.m.	25th October	2000	12:05 p.m.	depointing anomaly gyro 6 failure
17th January	2001		5th February	2001		gyro 1 failure Satellite in safe mode

TABLE 2 ERS-2 Scatterometer anomalies in the Doppler Compensation monitoring

Date start	Year	Date stop	Year	Reason
26th September	1996	27th September	1996	Missing on-board Doppler coefficient (after cal. DC converter test period)
6th June	1998	7th June	1998	No Yaw Steering Mode (after depointing anomaly)
2nd December	1998	3rd December	1998	Missing on-board Doppler coefficients (after AMI anomaly number 228)
16th February	2000	17th February	2000	Fine Pointing Mode (FPM) (due to AOCS mono-gyro qualification period)
14th April	2000	14th April	2000	Fine Pointing Mode (FPM)
5th July	2000	5th July	2000	Fine Pointing Mode (FPM) after instrument switch-on
27th September	2000	27th September	2000	Fine Pointing Mode (FPM) to upload AOCS software patch
2nd November	2000	2nd November	2000	Fine Pointing Mode (FPM)
5th December	2000	6th December	2000	Fine Pointing Mode (FPM) due to orbital manoeuvre
6th February	2001	30th March	2001	Extra Backup Mode (EBM) coarse attitude control
30th March	2001	17th June	2001	ZGM-EBM coarse attitude control
17th June	2001	21st August	2003	ZGM phase. Error in yaw angle not corrected in the ground segment processor. Data shall be reprocessed with ESACA.
24th March	2004	24th March	2004	Fine Pointing Mode (FPM) due to orbital manoeuvre
25th October	2004	27th October	2004	Series of orbital manoeuvres (OCM and FPM)
10th November	2004	11th November	2004	Intense geomagnetic storm
8th March	2005	8th March	2005	orbital manoeuvre (OCM)
11th March	2005	11th March	2005	orbital manoeuvre (FPM)

During the cycle 103 the Doppler compensation evolution was very stable (see Figure 3). The CoG of the compensated signal was around 0 Hz for the Fore and Aft antenna and around 200 Hz for the Mid antenna. The standard deviation of the CoG was around 1500 Hz for the Fore and Aft antenna and around 2700 Hz for the Mid antenna. The data gap shown in the plots for the period 5th – 6th March 2005 is due to an internal problem of the PCS monitoring process. Fast delivery data has been regularly disseminated to the users. The small variations on the CoG evolution on 8th and 11th March 2005 are due to orbital manoeuvres.

ERS-2 WindScatterometer: DOPPLER COMPENSATION Evolution (UWI)

Least-square poly. fit fore beam	Center of gravity = -123.9 +(0.0533)*day	Standard Deviation = 4401.3 +(-0.474)*day
Least-square poly. fit mid beam	Center of gravity = -788.1 +(0.3149)*day	Standard Deviation = 5884.9 +(-0.716)*day
Least-square poly. fit aft beam	Center of gravity = -347.8 +(0.1348)*day	Standard Deviation = 4582.5 +(-0.521)*day

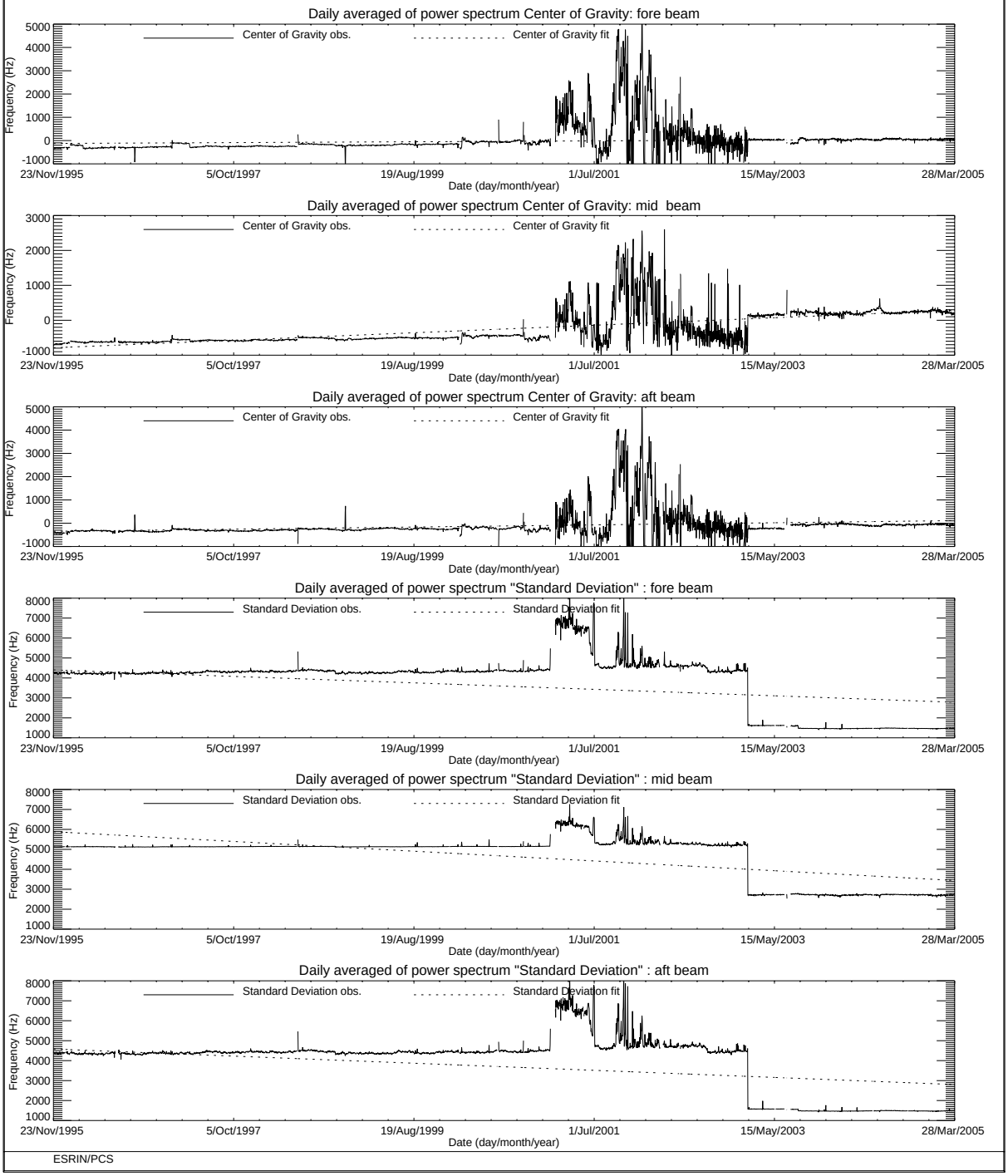

FIGURE 2 ERS-2 Scatterometer: Centre of Gravity and standard deviation of received power spectrum since the beginning of the mission.

ERS-2 WindScatterometer: DOPPLER COMPENSATION Evolution (UWI)

Least-square poly. fit fore beam	Center of gravity = 49.532 +(0.1571)*day	Standard Deviation = 1469.7 +(0.2019)*day
Least-square poly. fit mid beam	Center of gravity = 216.76 +(-0.563)*day	Standard Deviation = 2695.4 +(1.1839)*day
Least-square poly. fit aft beam	Center of gravity = -60.23 +(-0.239)*day	Standard Deviation = 1476.3 +(0.1860)*day

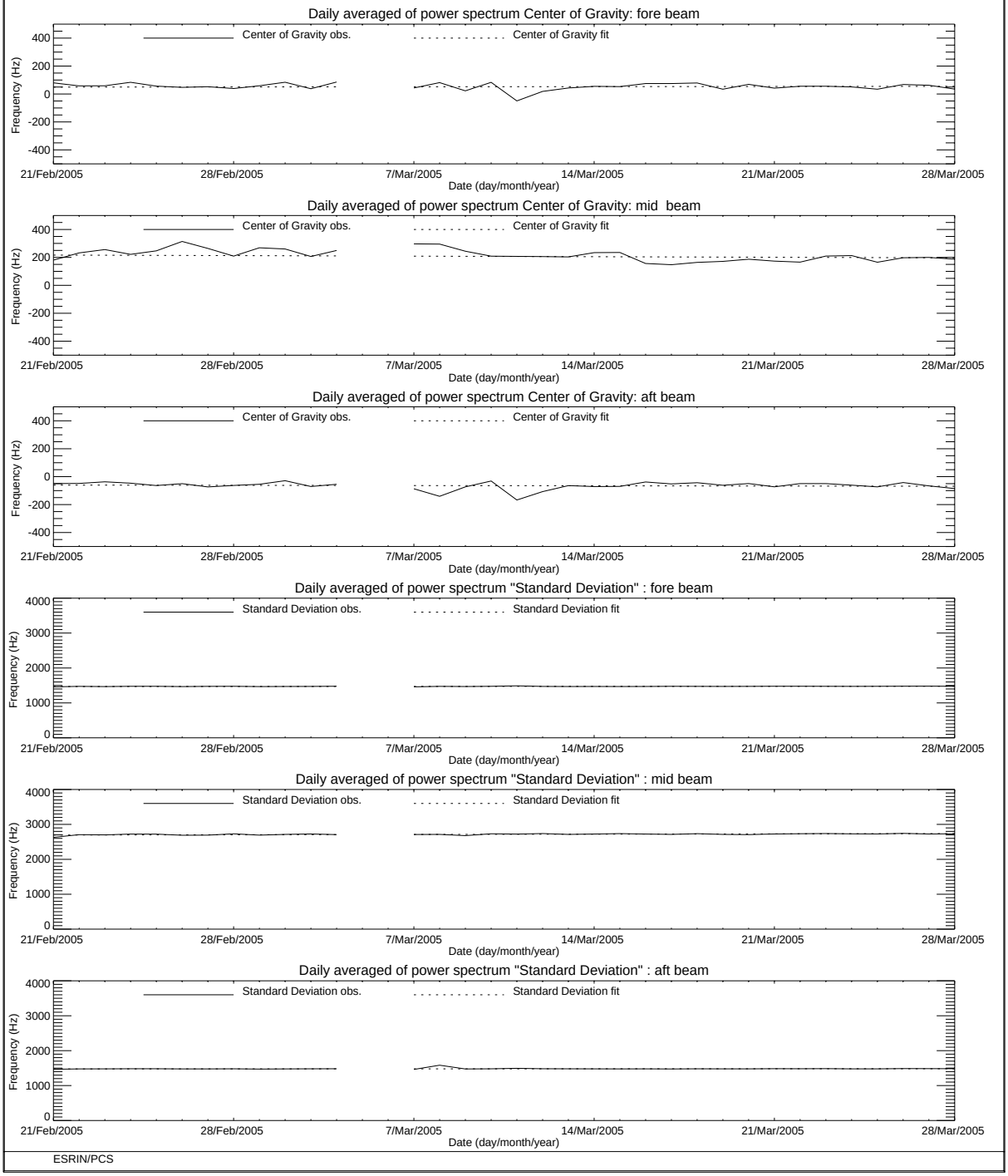

FIGURE 3 ERS-2 Scatterometer: Centre of Gravity and standard deviation of received power spectrum during the cycle 103.

3.2 Noise power level I and Q channel

The results of the monitoring are shown in Figure 4 (long-term) and Figure 5 (cycle 102). The first set of three plots presents the noise power evolution for the I channel while the second set shows the Q channel. From the plots one can see that the noise level is more stable in the I channel than in the Q one. The I and Q receivers are inside the same box and any external interference should affect both channel. The fact that the receivers are closer to the ATSR-GOME electronics could have some impact but there is no clear explanation on that behavior. From 5th December 1997 until November 1998 some high peaks appear in the plots. These high values for the daily mean are due to the presence for these special days of a single UWI product with an unrealistic value in the noise power field of its Specific Product Header. The analysis of the raw data used to generate these products lead in all cases to the presence of one source packet with a corrupted value in the noise field stored into the source packet Secondary Header. The reason why noise field corruption is beginning from 5th December 1997 and last until November 1998 is at present unknown. It is interesting to note that at the beginning of December 1997, we started to get as well the corruption of the Satellite Binary Times (SBTs) stored in the EWIC product. The impact in the fast delivery products was the production of blank products starting from the corrupted EWIC until the end of the scheduled stop time. A change in the ground station processing in March 1998 overcame this problem.
Since 9th August 1998 until March 2000 some periods with a clear small instability in the noise power have been recognized, Table 3 gives the detailed list.

TABLE 3 ERS-2 Periods with instability in the noise power

Start date	Stop date	Year
9th August	26th October	1998
29th November	6th December	1998
23rd December	24th December	1998
7th June	10th June	1999
17th August	22nd August	1999
8th September	9th September	1999
3rd October	8th October	1999
16th October	18th October	1999
26th October	28th October	1999
25th December	2nd January	2000
10th February	11th February	2000
19th March	26th March	2000

To better understand the instability of the noise power the PCS has carried out investigations in the Scatterometer raw data (EWIC) to compute the noise power with more resolution. The result is that for the orbits affected by the instability the noise power had a decrease of roughly 0.7 dB for the fore and aft signals and a decrease of roughly 0.6 dB in the mid beam case (see the report for the cycle 42). The decrease of the noise power during the orbits affected by the instability is comparable with the decrease of the internal calibration level that occurred during the same orbits. The reason of this instability (linked to the AMI anomalies) is still unknown. On 28th February 2003 the Scatterometer receiver gain has been increased by 3 dB to optimize the usage of the on-board ADC converter. This explains the increase of the noise for the Fore and Aft beam channel. For the mid beam channel the noise still remains not measurable. The evolution of the noise power during the cycle 103 was stable (see Figure 5). The daily average for the Fore and Aft beam noise is around 1.7 ADC (I) and around 1.6 ADC (Q) respectively. For the Mid beam the noise is not measurable. The data gap shown in

the plots for the period 5th – 6th March 2005 is due to an internal problem of the PCS monitoring process. Fast delivery data has been regularly disseminated to the users.

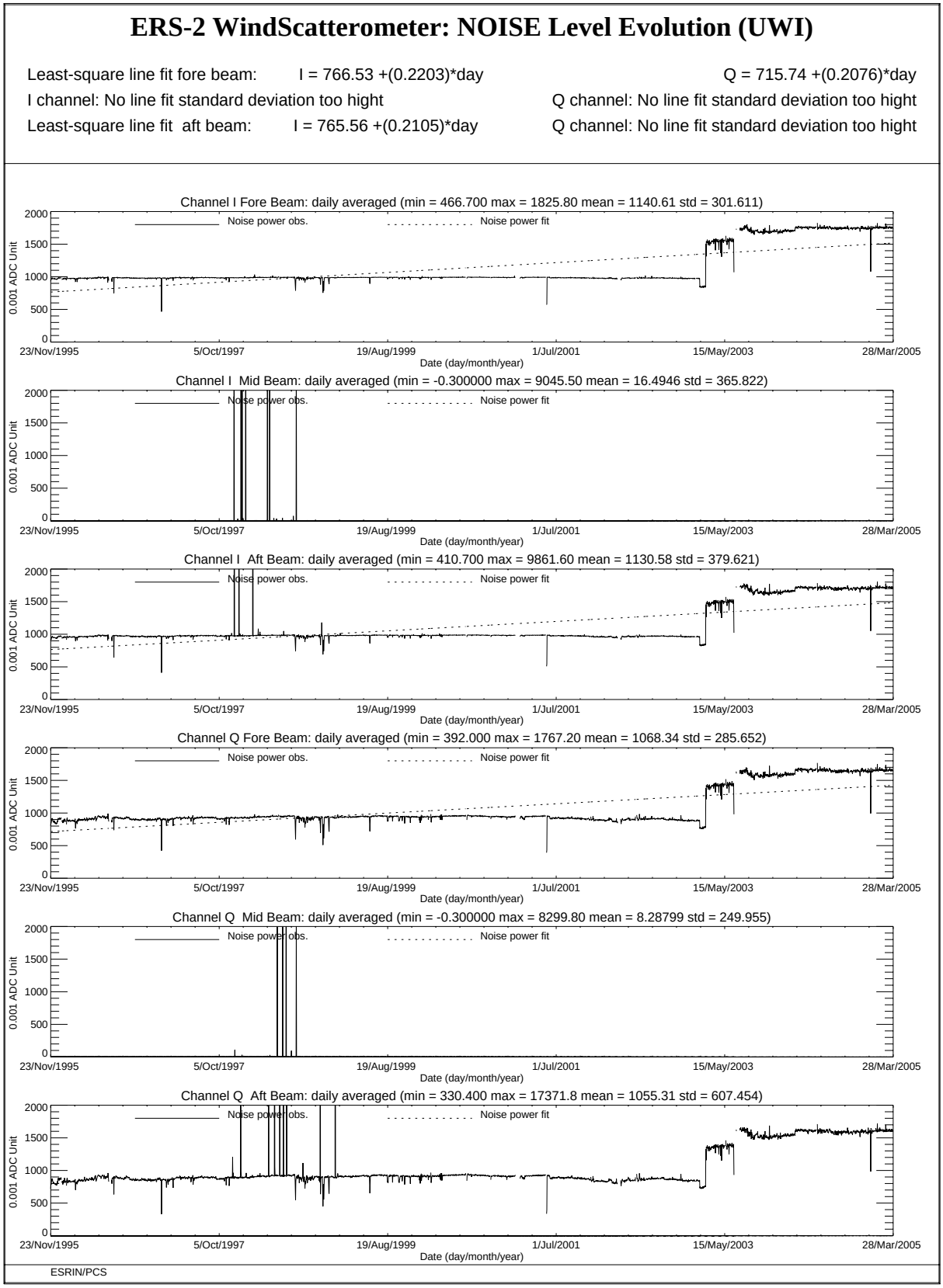

FIGURE 4 ERS-2 Scatterometer: noise power I and Q channel since the beginning of the mission.

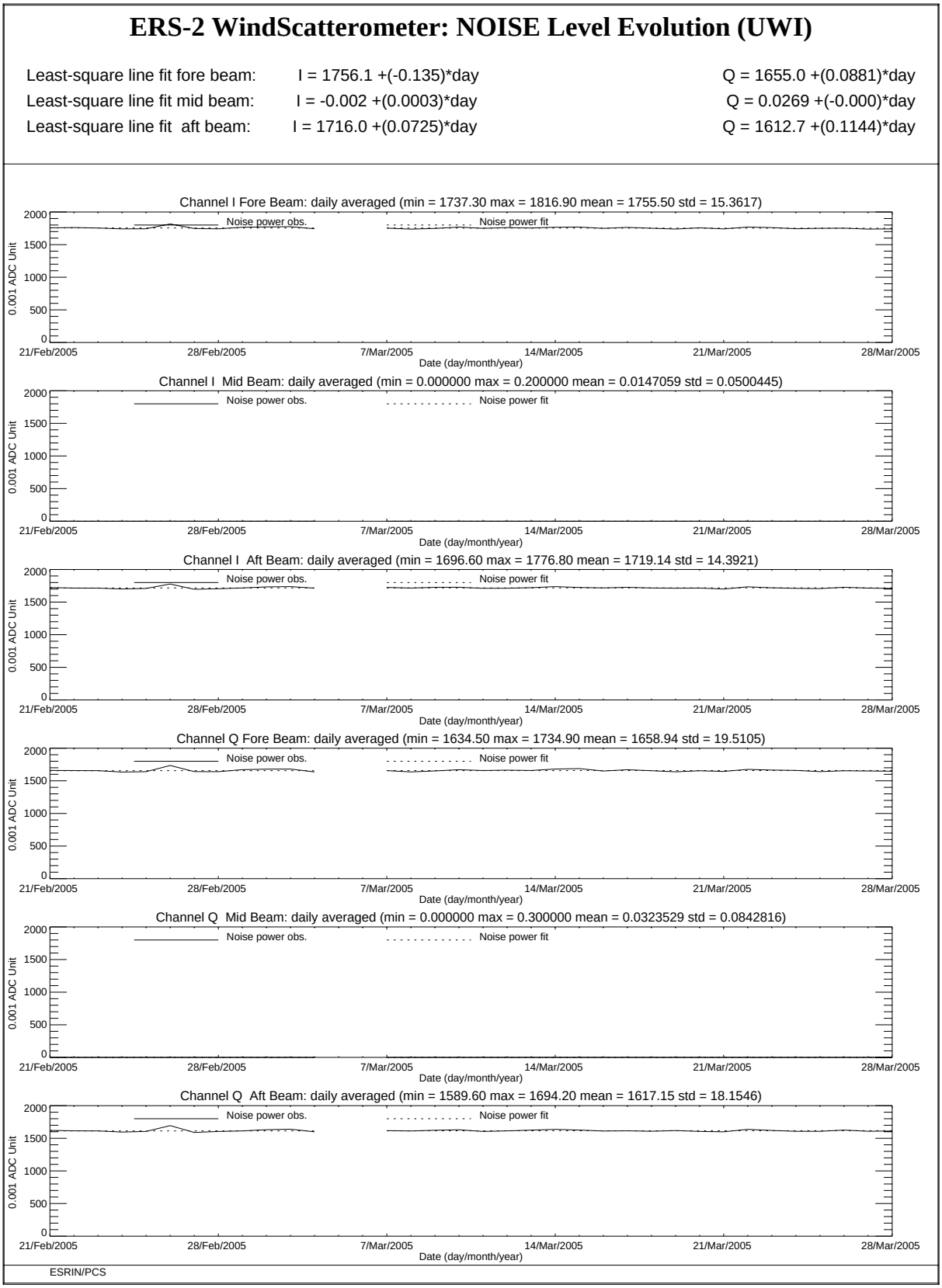

FIGURE 5 ERS-2 Scatterometer: noise power I and Q channel for cycle 103.

3.3 Power level of internal calibration pulse

For the internal calibration level, the results are shown in Figure 6 (long-term) and Figure 7 (cycle 103). The high value of the variance in the fore beam until August, 12th 1996 is due to the ground processing. In fact all the blank source packets ingested by the processor were recognized as Fore beam source packets with a default value for the internal calibration level. The default value was applicable for ERS-1 and therefore was not appropriate for ERS-2 data processing. On August 12th, 1996 a change in the ground processing LUT overcame the problem. Since the beginning of the mission a power decrease is detected. The power decrease is regular and affects the AMI when it is working in wind-only mode, wind/wave mode and image mode indifferently. The average power decrease is around 0.08 dB per cycle (0.0022 dB/day) and is clearer after August, 6th 1996 when the calibration subsystem has been changed. The reason of the power decrease is because the TWT is not working in saturation, so that a variation in the input signal is visible in the output. The variability of the input signal can be two-fold: the evolution of the pulse generator or the tendency of the switches between the pulse generator and the TWT to reset themselves into a nominal position. These switches were set into an intermediate position in order to put into operation the Scatterometer instrument (on 16th November 1995). To compensate for this decrease, on 26th October 1998 (cycle 37) 2.0 dB were added to the Scatterometer transmitted power and on 4th September 2002 (cycle 77) were added 3.0 dB. On 28th February 2003 (cycle 82) the Scatterometer receiver gain was increased by 3 dB to improve the usage of the on-board ADC converter. These events are clearly displayed by the large steps show in Figure 6.
Since 9th August 1998 until March 2000 the internal calibration level shows instability after an AMI or platform anomaly (see reports from cycle 35 to cycle 52). This instability is very well correlated with the fluctuations observed in the noise power. On 13th July 2000 a high peak (+3.5 dB) was detected in the transmitted power. This event has been investigated deeply by PCS and ESOC. The results of the analysis are reported in the technical note “ERS-2 Scatterometer: high peak in the calibration level” available in the PCS. The high transmitted power was detected after an arcing event which occurred inside the HPA. After that event the transmitted power had an average increase of roughly 0.14 dB.

During the cycle 103 the mean transmitted power evolution was very stable. The mean decrease has been very small (0.03 dB per cycle), it was 0.14 dB for cycle 102. The data gap shown in the plots for the period 5th – 6th March 2005 is due to an internal problem of the PCS monitoring process. Fast delivery data has been regularly disseminated to the users.

ERS-2 WindScatterometer: Internal CALIBRATION Level Evolution (UWI)

Least-square polynomial fit fore beam	gain (dB) per day -0.0001	1062.48 +(-0.0191443)*day
Least-square polynomial fit mid beam	gain (dB) per day -0.0001	314.133 +(-0.00540559)*day
Least-square polynomial fit aft beam	gain (dB) per day -0.0001	1050.61 +(-0.0185327)*day

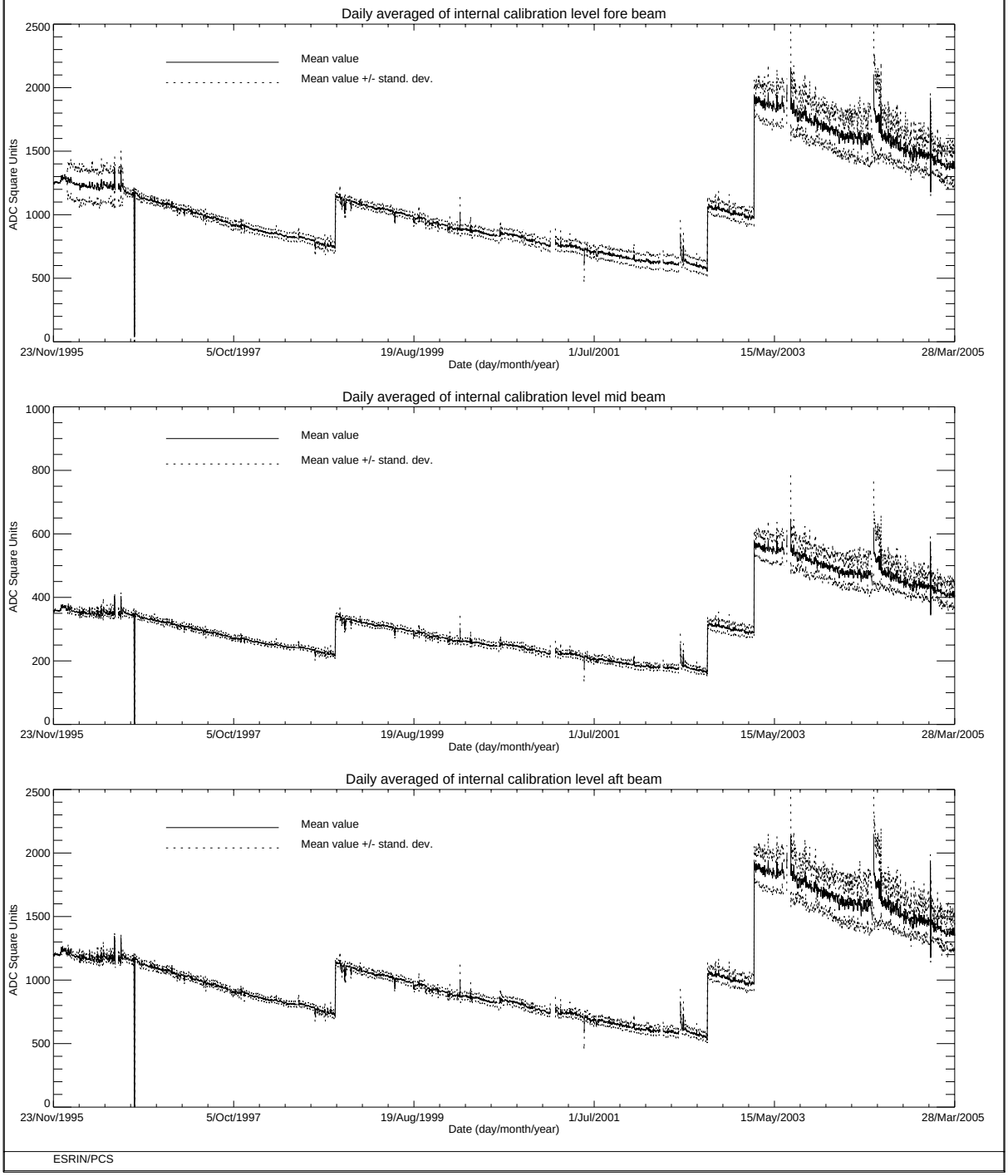

FIGURE 6 ERS-2 Scatterometer: power of internal calibration pulse since the beginning of the mission.

ERS-2 WindScatterometer: Internal CALIBRATION Level Evolution (UWI)

Least-square polynomial fit fore beam	gain (dB) per day 0.0009	1376.19 +(0.287250)*day
Least-square polynomial fit mid beam	gain (dB) per day 0.0010	406.922 +(0.0934226)*day
Least-square polynomial fit aft beam	gain (dB) per day 0.0009	1366.04 +(0.294720)*day

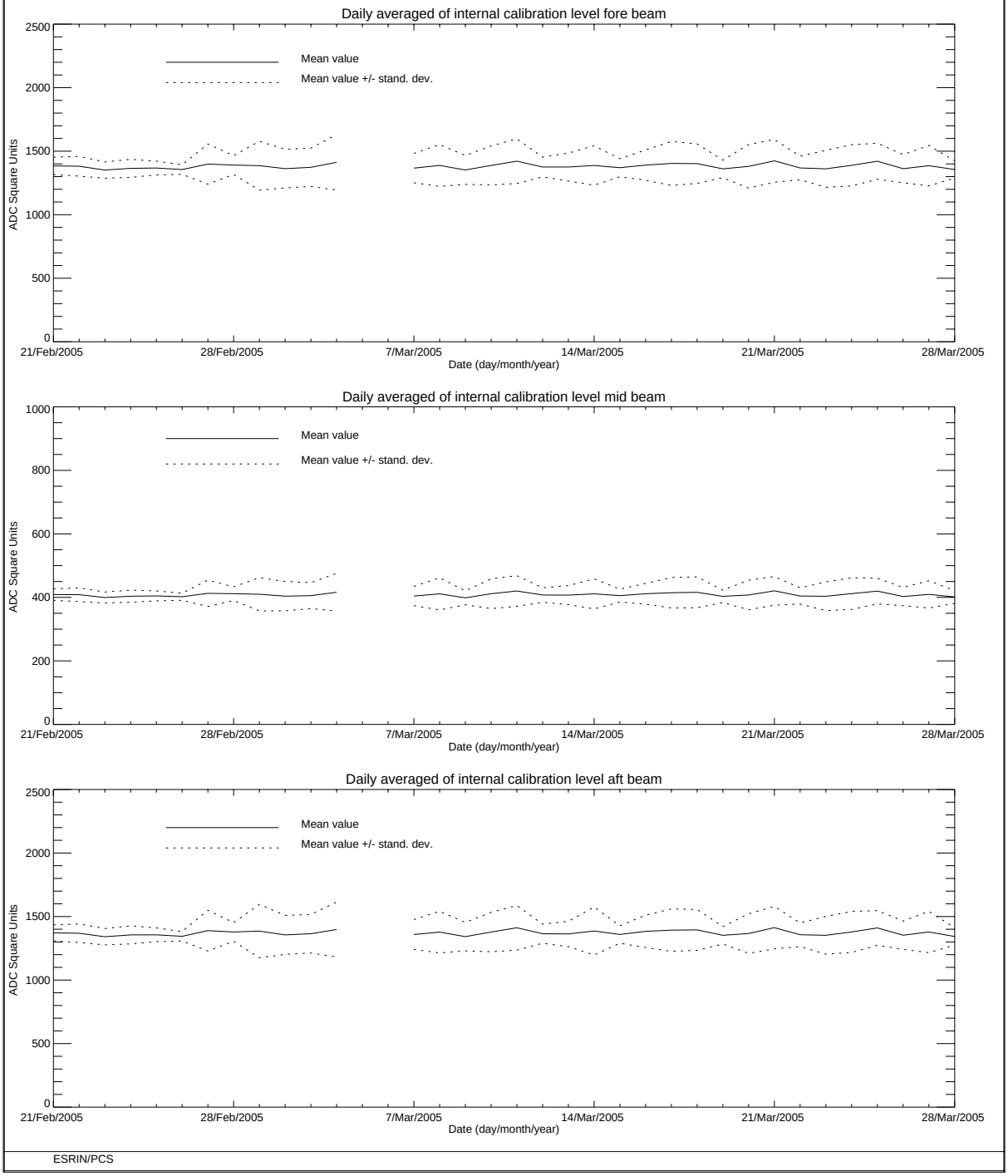

FIGURE 7 ERS-2 Scatterometer: power of internal calibration level cycle 103.

4 Products performance

The PCS carries out a quality control of the winds generated from the WSCATT data. External contributions to this quality control (from ECMWF) are also reported in this chapter.

4.1 Products availability

One of the most important points in the monitoring of the products performance is their availability. The Scatterometer is a part of ERS payload and it is combined with a Synthetic Aperture Radar (SAR) into a single Active Microwave Instrument (AMI). The SAR users requirements and the constraints imposed by the on-board hardware (e.g. amount of data that can be recorded in the on-board tape) set rules in the mission operation plan.

The principal rules that affected the Scatterometer instrument data coverage are:
• Over the Ocean the AMI is in wind/wave mode (Scatterometer with small SAR imagettes acquired every 30 sec.) and the ATSR-2 is in low rate data mode.
• Over the Land the AMI is in wind only mode (only Scatterometer) and the ATSR-2 is in high rate mode. (Due to on board recorder capacity, ATSR-2 in high rate is not compatible with SAR wave imagettes acquisitions.) This strategy preserves the Ocean mission.
• The SAR images are planned as consequence of users' request.

Moreover:

- since July 16th 2003 the ERS-2 Low Rate mission is continued within only the visibility of ESA ground stations over Europe, North Atlantic, the Arctic and western North America. The reason was the failure of both on-board tape recorders.
- During the cycles 64 – 92 (June 2001 since 25th February 2004) the AMI instrument was operated in wind/wave mode also over the land. The reason was because the SAR wave data was used to estimate the satellite mispointing along the full orbit. Since 25th February onwards the nominal mission scenario has been resumed, with the AMI instrument in wind only mode over the land (and consequently ATSR was operated again in High Rate over land). The mispointing performances (in particular the yaw error angle) along the full orbit are computing by analyzing the Scatterometer data.

In order to maximize the data coverage, after the on-board tape recorder failure, an upgrade of the ERS ground segment acquisition scenario has been performed.
In that framework the following has been implemented:

- Since September 7th 2003 the ground station in Maspalomas, Gatineau and Prince Albert are acquiring and processing data for all the ERS-2 satellite passes within the station visibility (apart from passes for which other satellites have an higher priority).
- To further increase the wind coverage of the North Atlantic area, since December 8th, 2003 is operative a new ground Station in West Freugh (UK) and data from this new station are available to the user since mid January 2004. Due to its location, the West Freugh acquisitions have some overlap with those from three other ESA stations, Kiruna, Gatineau or Maspalomas. The station overlap depends on the relative orbit of the satellite. Consequentially, overlapping wind Scatterometer LBR data may be included in two products. Since the two products are generated at different ground stations the overlap

may not be completely precise, with a displacement up to 12 Km and slight differences in the wind data itself.

- Since March, 3rd 2004, Matera station is acquiring low rate bit data for all the passes for which is planned a SAR acquisition. Gome science data are produced and disseminated to users, Radar Altimeter data, Wave data and Scatterometer data are recorded on tapes and will be available off-line for re-processing. This means for the Scatterometer data coverage a very limited improvement due to the fact that are acquired only passes with some SAR activity.
- Since February 2005 a new acquisition station in Miami (US) is in operations. This will let a full coverage of the Gulf of Mexico and part of the Pacific Ocean on the west Mexico coast.

Figure 8 shows the AMI operational modes for cycle 103. Each segment of the orbit has different color depending on the instrument mode: brown for wind only mode, blue for wind-wave mode and green for image mode. The red and yellow colors correspond to gap modes (no data acquired). For cycle 103 the percentage of the ERS-2 AMI activity is shown in table 4. The values are within the nominal range.

TABLE 4 ERS-2 AMI activity (cycle 103)

Ami Mode	Ascending passes	Descending passes
Wind and Wind-Wave	**92.64 %**	**81.65%**
Image	**2.41 %**	**12.37 %**
Gap and others	**4.95 %**	**5.98 %**

Table 5 reports the major data lost due to the test periods, AMI and satellite anomalies or ground segment anomalies occurred after 6th August, 1996 (before that day for many times data were not acquired due to the DC converter failure).

TABLE 5 ERS-2 Scatterometer mission major data lost after 6th, August 1996

Start date	Stop Date	Reason
September 23rd, 1996	September 26th , 1996	ERS 2 switched off due to a test period
February 14th , 1997	February 15th , 1997	ERS 2 switched off due to a depointing anomaly
June 3rd, 1998	June 6th, 1998	ERS 2 switched off due to a depointing anomaly
November 17th , 1998	November 18th , 1998	ERS 2 switched off to face out Leonide meteor storm
September 22nd 1999	September 23rd 1999	ERS 2 switched off due to Year 2000 certification test
November 17th , 1999	November 18th , 1999	ERS 2 switched off to face out Leonide meteor storm
December 31st ,1999	January 2nd , 2000	ERS 2 switched off Y2K transition operation
February 7th ,2000	February 9th , 2000	ERS 2 switched off due to new AOCS s/w up link
June 30th , 2000	July 5th , 2000	ERS 2 Payload switched off after RA anomaly
July 10th , 2000	July 11th , 2000	ERS 2 Payload reconfiguration
October 7th , 2000	October 10th 2000	ERS 2 Payload switched off after AOCS anomaly
January 17th , 2001	February 5th , 2001	ERS 2 Payload switched off due to AOCS anomaly
May 22nd , 2001	May 24th , 2001	ERS 2 Payload switched off due to platform anomaly
May 25th , 2001	May 25th , 2001	AMI switched off due thermal analysis
November 17th , 2001	November 18th , 2001	ERS 2 switched off to face out Leonide meteor storm
November 27th , 2001	November 28th , 2001	ERS 2 payload off due to 1Gyro Coarse Mode commissioning
March 8th , 2002	March 20th , 2002	ERS 2 payload unavailability after RA anomaly
May 19th ,2002	May 24th 2002	AMI switched off due to arc events
May 24th , 2002	May 28th , 2002	AMI partially switched off due to arc events
May 31st 2002	June 3rd 2002	Gatineau orbits partially acquired due to antenna problem
June 4th , 2002	June 5th , 2002	AMI partially switched-off due to arc events

July 25th , 2002	July 25th , 2002	AMI switched off HPA voltage too low
September 11th , 2002	September 11th , 2002	AMI switched off macrocommand transfer error
November 17th, 2002	November 18th, 2002	ERS-2 switched off to face out Leonide meteor storm
December 9th , 2002	December 10th , 2002	IDHT anomaly no data recorded on board
December 20th , 2002	December 20th 2002	IDHT anomaly no data recorded on board
January 14th , 2003	January 14th, 2003	IDHT anomaly no data recorded on board
May 6th , 2003	May 19th , 2003	AMI off due to bus reconfiguration
June 22nd , 2003	July 16th ,2003	IDHT recorders test no data acquired
Since July 16th ,2003		Regional Mission Scenario. Data available only within the visibility of ESA ground station
May 21st, 2004	May 25th, 2004	AMI in refuse mode due to excessive HPA arcing
June 22nd ,2004	June 22nd , 2004	AMI in refuse mode due to excessive HPA arcing
September 23rd, 2004	September 24th, 2004	AMI switched down
December 16th, 2004	December 17th, 2004	AMI memory test
December 26th, 2004	December 26th, 2004	IDHT anomaly. No data acquired
December 27th, 2004	December 28th, 2004	Payload off due to on board anomaly
January 23rd , 2005	January 23rd , 2005	AMI switched down (00.51 a.m. – 1.26 p.m.)
January 28th , 2005	January 28th , 2005	AMI switched down (01.29 a.m. – 10.39 a.m.)
February 26th , 2005	February 26th , 2005	AMI switched down (01.20 a.m. – 12.37 a.m.)
March 11th , 2005	March 11th , 2005	AMI switched down (02.43 p.m. – 05.41 p.m.)

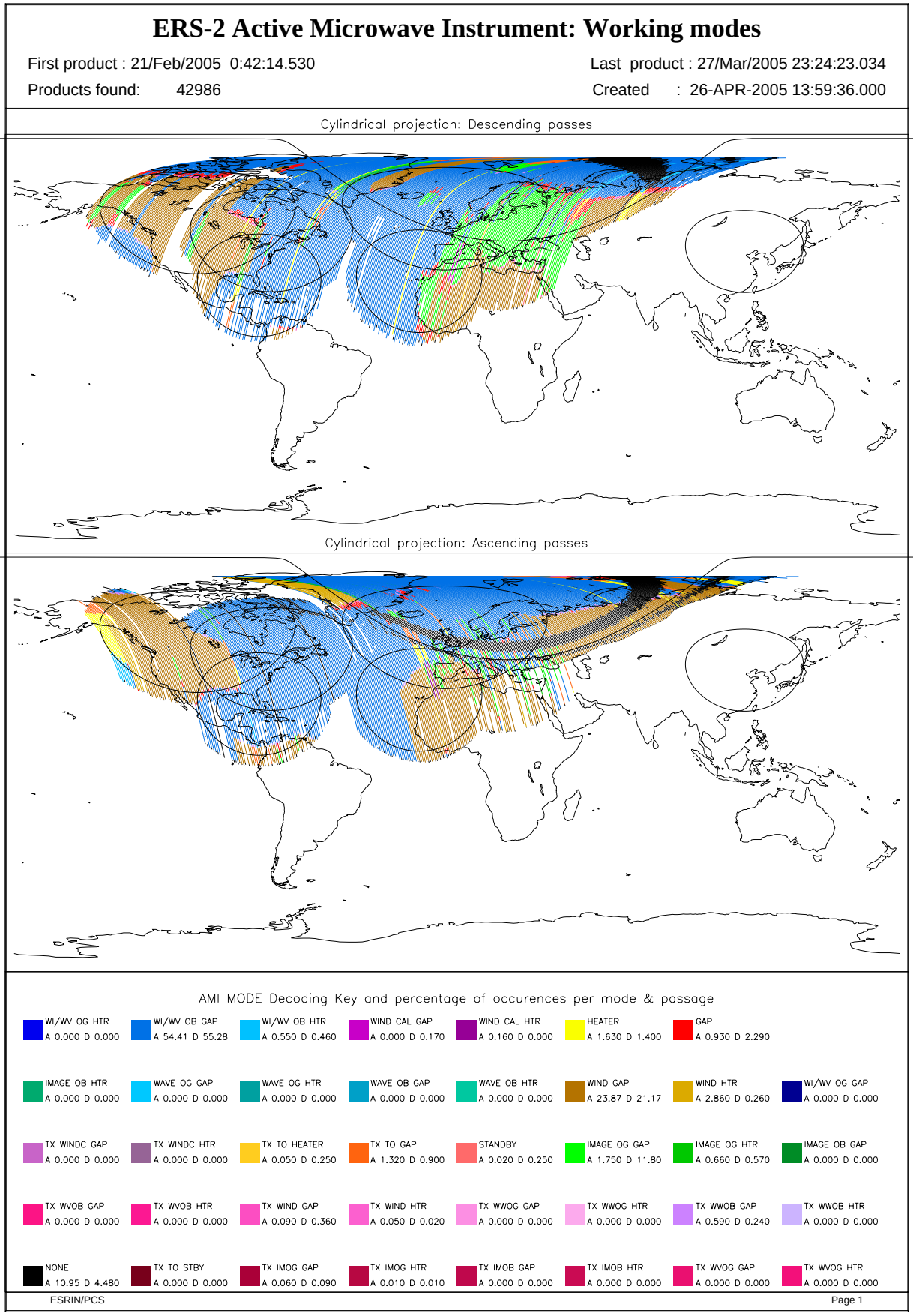

FIGURE 8 ERS-2 AMI activity during cycle 103.

4.2 PCS Geophysical Monitoring

The routine analysis is summarized in the plots of figure 9; from top to bottom:

• the monitoring of the valid sigma-nought triplets per day.
• the evolution of the wind direction quality. The ERS wind direction (for all nodes and only for those nodes where the ambiguity removal has worked properly) is compared with the ECMWF forecast. The plot shows the percentage of nodes for which the difference falls in the range -90.0, +90.0 degrees.
• the monitoring of the percentage of nodes whose ambiguity removal works successfully.
• the comparison of the wind speed deviation: (bias and standard deviation) with the ECMWF forecast.

The results since August 6th, 1996 until the beginning of the operation with the Zero Gyro Mode (ZGM) in January 2001 can be summarized as:
• High quality wind products has been distributed since Mid March 1996 (end of calibration and validation phase)
• The number of valid sigma-nought distributed per day was almost stable with a small increase after June 29th, 1999 due to the dissemination in fast delivery of the data acquired in the Prince Albert station (Canada).
• The wind direction is very accurate for roughly 93% of the nodes, the ambiguity removal processing successfully worked for more than 90.0% of the nodes.
• The UWI wind speed shows an absolute bias of roughly 0.5 m/s and a standard deviation that ranges from 2.5 m/s to 3.5 m/s with respect to the ECMWF forecast.
• The wind speed bias and its standard deviation have a seasonal pattern due to the different winds distribution between the winter and summer season.
• Two important changes affect the speed bias plot.
• the first is on June 3rd , 1996 due to the switch from ERS-1 to ERS-2 data assimilation in the meteorological model.
• the second which occurred at the beginning of September 1997, is due to the new monitoring and assimilation scheme in ECMWF algorithms (4D-Var).
• Since 19th April 1999 two set of meteo-table (meteorological forecast centred at 00:00 and 12:00 of each day) are used in the ground processing. This allowed the processing of wind data with 18 and 24 hours meteorological forecast instead of the 18, 24, 30 36 hours forecast. The comparison between data processed with the 18-24 hours forecast instead of 30-36 hours forecast shown an increase in the number of ambiguity removed nodes with a neutral impact in the daily statistics.
• The mono-gyro AOCS configuration (see report for cycle 50) that was operative from 7th February 2000 to 17th January 2001 did not affect the wind data performance.
During the Zero Gyro Mode (ZGM) phase the dissemination of the fast delivery Scatterometer data to the users has been interrupted on 17th January 2001 due to degraded quality in sigma noughts and winds. The satellite attitude in ZGM is slightly degraded and the "old" ground processor was not able to produce calibrated data anymore. For that reason a re-design of the entire ground processing has been carried out and since August 21st 2003 the new processor named ERS Scatterometer Attitude Corrected Algorithm (ESACA) is operative in all the ESA ground station and data was redistributed to the user.
Although for a long period data was not distributed, the PCS has monitored the data quality (as shown in Figure 9) and the results during that period can be summarized as:

At the beginning of the ZGM (January 2001 - end July 2001) the number of valid nodes has clear drop from 190000 per day to 9000 per day. This because the satellite attitude was strong degraded and the received signal had a very high Kp figure (in particular for the far range nodes). For the valid nodes, due to no calibrated sigma nought, the quality of the wind was very poor, the distance from the cone was high and the wind speed bias was above 1.5 m/s.
At the end of July 2001 the ZGM has been tuned and the satellite attitude had an improvement. This explains the increase of the number of valid nodes (returned around the nominal level) and the improvements in the wind speed bias (around 0.5 m/s).
On 4th February 2003, a beta version of the new ESACA processor has been put in operation in Kiruna for validation and the monitoring of the data quality has been done only for the new ESACA data. The number of valid nodes slight decreased because Kiruna station process only 9 of 14 orbits per day. The wind speed direction deviation had a clear improvement because ESACA implements a new ambiguity removal algorithm (MSC) and the ambiguity removal rate is now stable at 100% (the MSC is able to remove ambiguity for all the nodes). The wind speed bias had a clear drop from 0.5 to -0.5 m/s. That value is closer to the nominal one (around -0.2 m/s). As reported in the previous cyclic reports the beta version of ESACA had some calibration problem for the near range nodes and this explains why the data quality does not match exactly the one obtained in the nominal YSM. That problem has been overcome with the final release of the ESACA processor put into operation on August 21st 2003. On June 22nd the failure of the on-board tape recorder discontinued the ERS global mission (see section 4.1) and this explains the low number of valid nodes available after that day.
The performances of ESACA winds delivered between August 2003 and September 2004 are affected by land contamination. Around costal zones many Sea nodes have a strong contribution of Land backscattering and the retrieved wind is not correct. An optimization of the Land/Sea flag in the ground processing has been carried out during the cycle 98. In the statistics computed by PCS on the fast delivered winds the Land contamination has been removed by using a refined Land/Sea mask. Also the ice contamination has been removed with a simple geographical filter. With these new setting the PCS statistics are very similar to the ones reported by ECMWF.

For cycle 103 the wind performances slightly degraded. The wind speed bias (UWI vs 18 or 24 hour forecast) was roughly 0.7 m/s (it was 0.6 m/s for cycle 102) and the speed bias standard deviation was around 1.8 m/s (it was 1.6 m/s for cycle 102). Those values are very similar to the ones computed by ECMWF. The fluctuation of the statistics is mainly due to the small amount of data available for each day. Since mid March 2005 onwards the numbers of valid triplets had increased. The reason was an improvement of the Yaw performances that had reduced the number of flagged nodes (those nodes are invalid in the PCS monitoring schema).

The wind direction deviation was good. The 98% of the nodes have a wind direction in agreement with the meteorological forecast.

The data gap shown in the plots for the period 5th – 6th March 2005 (see figure 10) is due to an internal problem of the PCS monitoring process. Fast delivery data has been regularly disseminated to the users

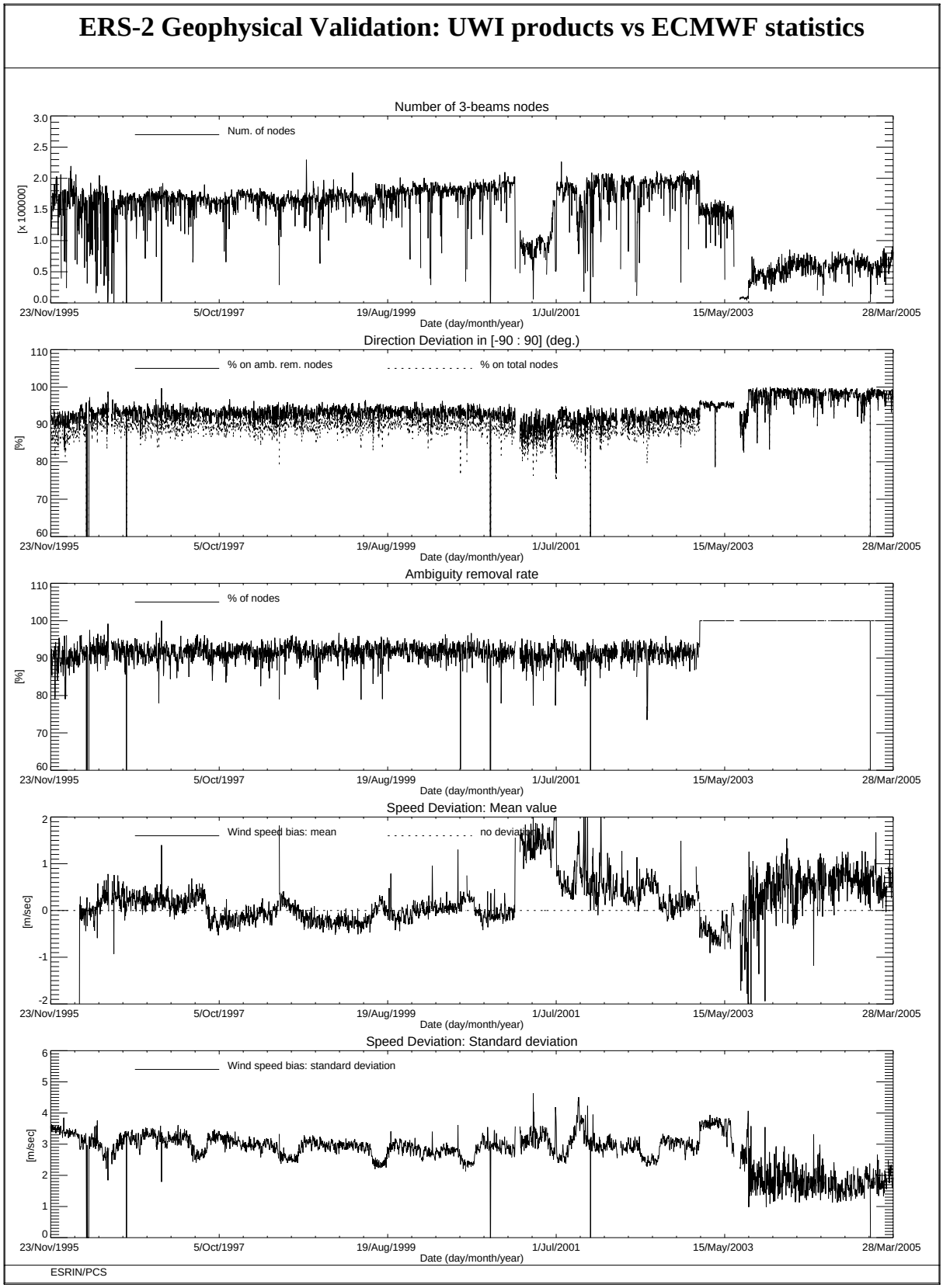

FIGURE 9 ERS-2 Scatterometer: wind products performance since the beginning of the mission.

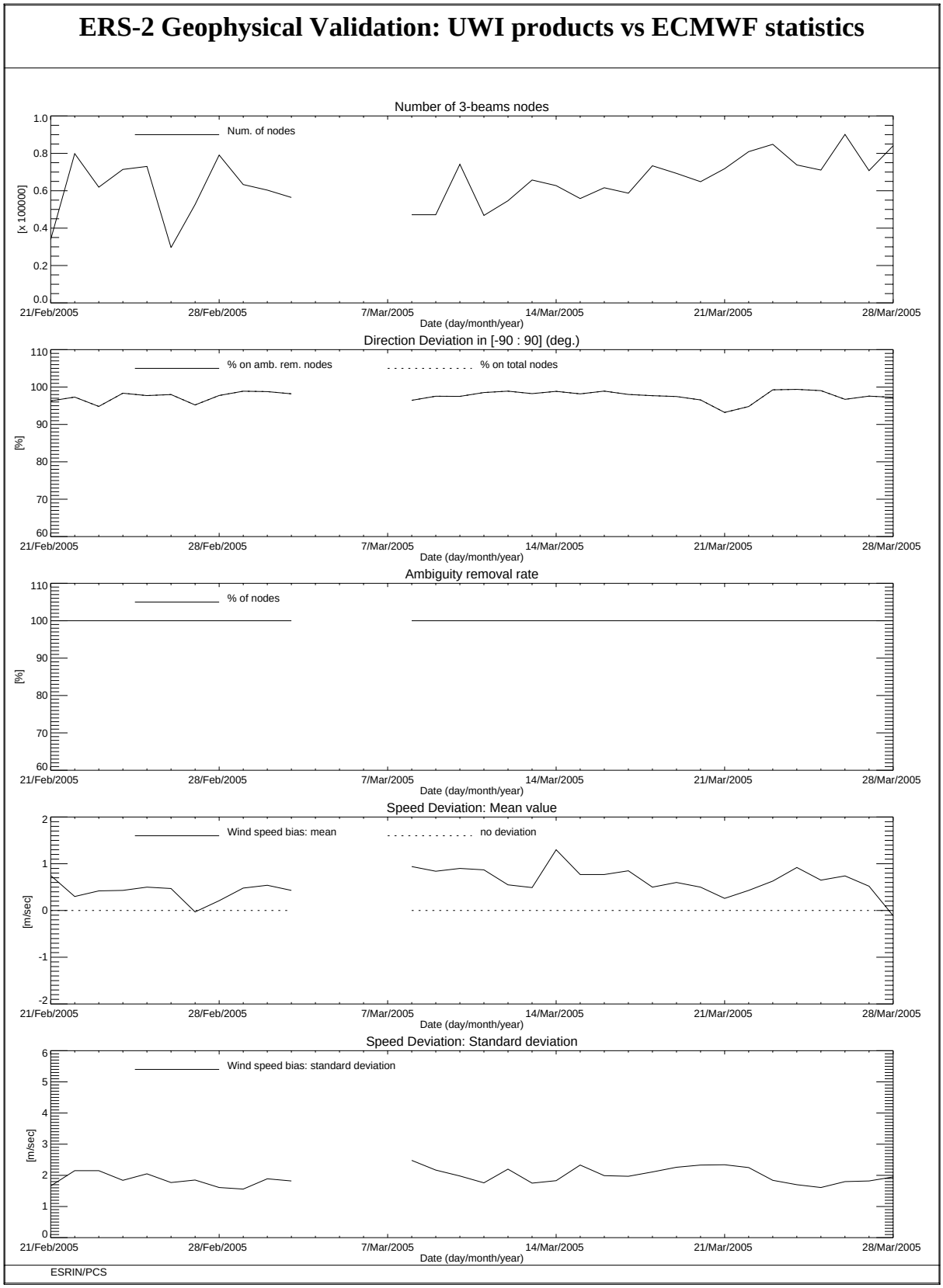

FIGURE 10 ERS-2 Scatterometer: wind products performance for cycle 103.

4.3 ECMWF Geophysical Monitoring

The quality of the UWI product was monitored at ECMWF for cycle 102. Results were compared to those obtained from the previous cycle, as well for data received during the nominal period in 2000 (up to cycle 59). No corrections for duplicate observations were applied.

During cycle 103 data was received between 21:04 UTC 21 February 2005 and 20:58 UTC 28 March 2005. No data was received for the 6-hourly data batch of 06 UTC 26 February 2005 (AMI instrument anomaly), 00 UTC 2 March 2005 and 00 UTC 3 March 2005.

Data is being recorded whenever within the visibility range of a ground station, leading for cycle 101 to a coverage of the North-Atlantic, part of the Mediterranean, the Gulf of Mexico, and to a small part of the Pacific north-west from the US and Canada (see Figure 12).

The asymmetry between the fore and aft incidence angles showed the development of several enhanced peaks, the largest occurring on 23 February 2005, 7 March 2005, 8 March 2005, and 11 March 2005. The k_p-yaw ESA flag was set accordingly. The events on 7 and 8 March coincided with an enhanced solar wind (source www.spaceweather.com).

Compared to cycle 102, the comparison of the UWI wind speed with ECMWF first-guess (FG) fields showed a similar relative standard deviation (1.56 m/s to 1.55 m/s). The relative bias has become more negative (from -0.65 m/s to -0.72 m/s). For winds based on CMOD5 the negative bias has grown as well (from -0.08 m/s to -0.18 m/s). Both relative bias levels and standard deviation are better to those for 2000 (see Figure 11).

Ocean calibration shows that both bias levels and internode differences are small and stable.
The performance of the UWI wind direction was highly reduced between 6 and 9 March 2005. For de-aliased CMOD4 winds this behavior was not observed, indicating a temporarily problem in the ESACA de-aliasing software.

The cycle-averaged evolution of performance relative to ECMWF first-guess (FG) winds is displayed in Figure 11. Figure 12 shows global maps of the over cycle 102 averaged UWI data coverage and wind climate, Figure 13 for performance relative to FG winds.

The ECMWF assimilation system was not changed during cycle 103.

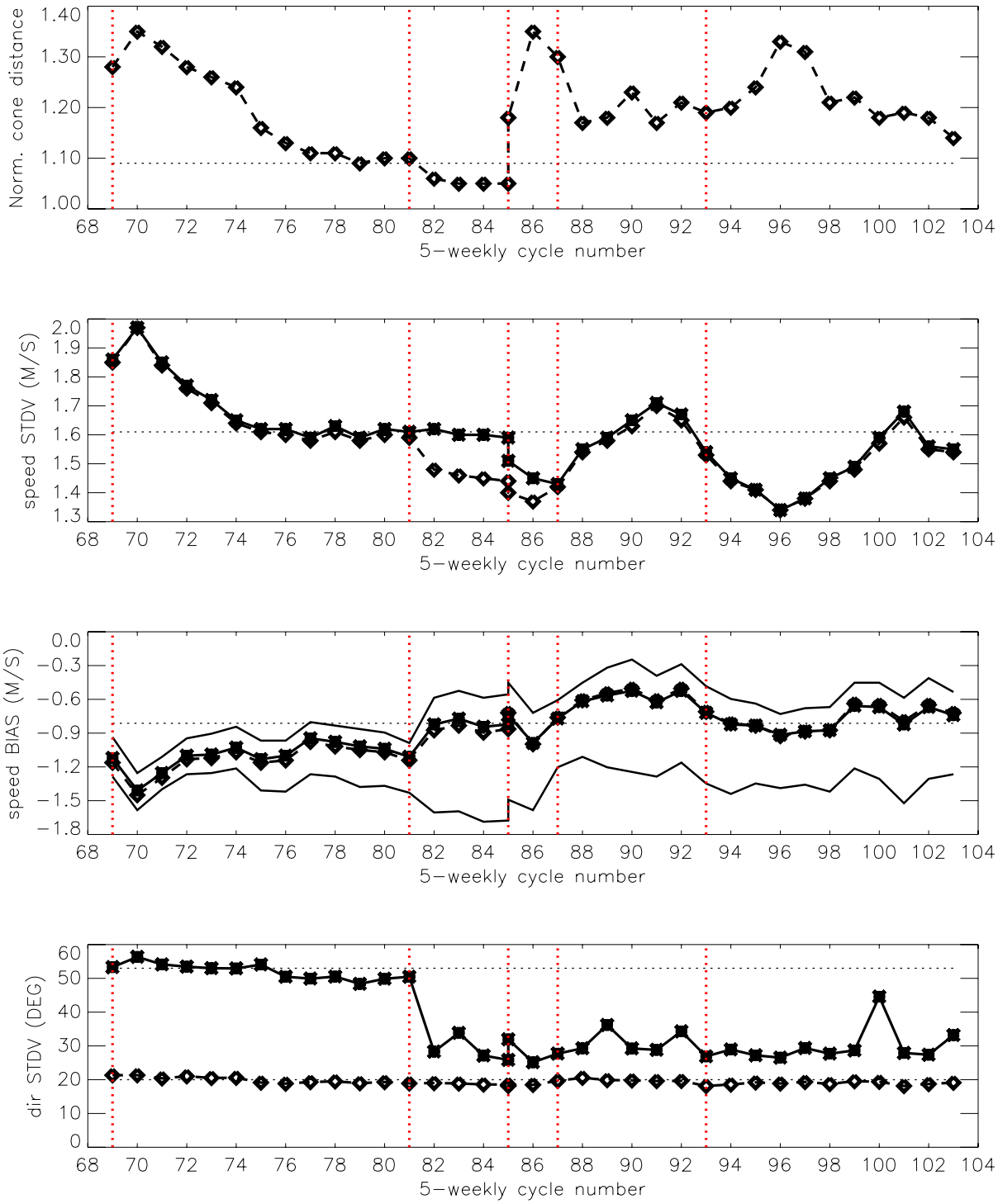

FIGURE 11 Evolution of the performance of the ERS-2 Scatterometer averaged over 5-weekly cycles from 12 December 2001 (cycle 69) to 28 March 2005 (end cycle 103) for the UWI product (solid, star) and de-aliased winds based on CMOD4(dashed, diamond). Results are based on data that passed the UWI QC flags. For cycle 85 two values are plotted; the first value for the global set, the second one for the regional set. Dotted lines represent values for cycle 59 (5 December 2000 to 17 January 2001),i.e. the last stable cycle of the nominal period. From top to bottom panel are shown the normalized distance to the one (CMOD4 only) the standard deviation of the wind speed compared to FG winds, the corresponding bias(for UWI winds the extreme inter-node averages are shown as well),and the standard deviation of wind direction compared to FG.

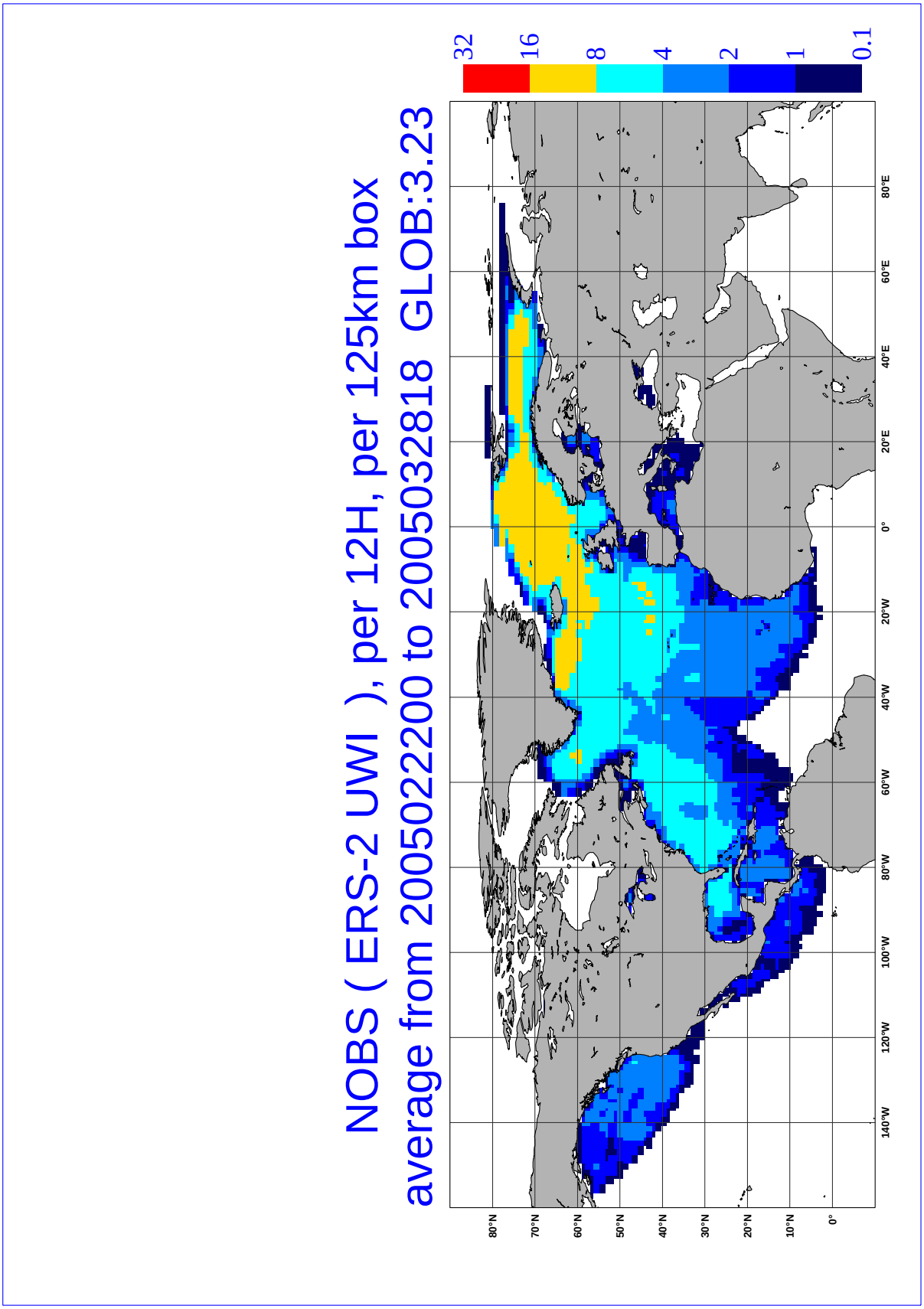
NOBS (ERS-2 UWI), per 12H, per 125km box
average from 2005022200 to 2005032818 GLOB:3.23
32
16
8
4
2
1
0.1
80°E
60°E
40°E
20°E
0°
20°W
40°W
60°W
80°W
100°W
120°W
140°W
80°N
70°N
60°N
50°N
40°N
30°N
20°N
10°N
0°

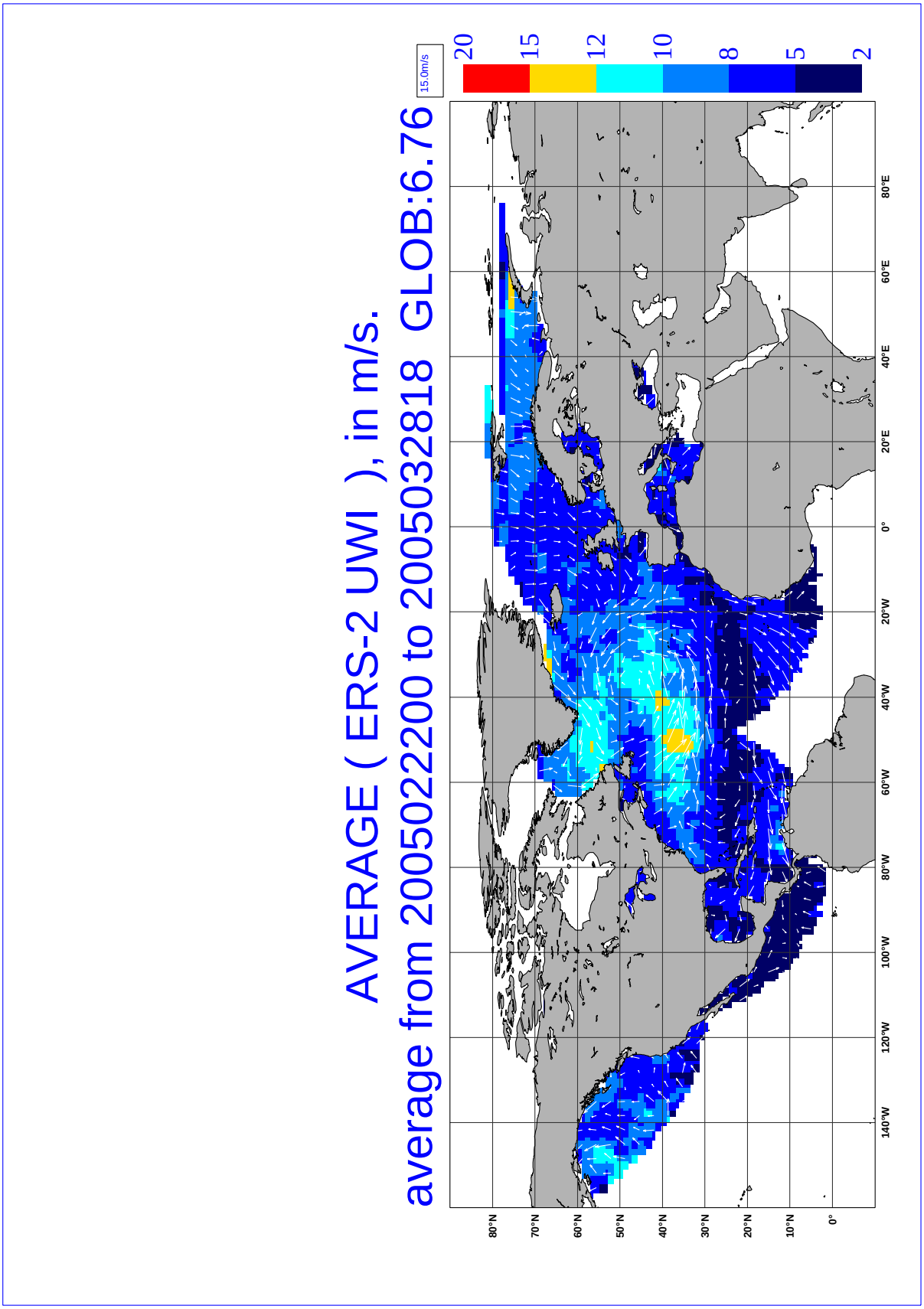

FIGURE 12 Average number of observations per 12H and per 125km grid box (top panel) and wind-climate (lower panel) for UWI winds that passed the UWI flags QC and a check on the collocated ECMWF land and sea-ice mask.

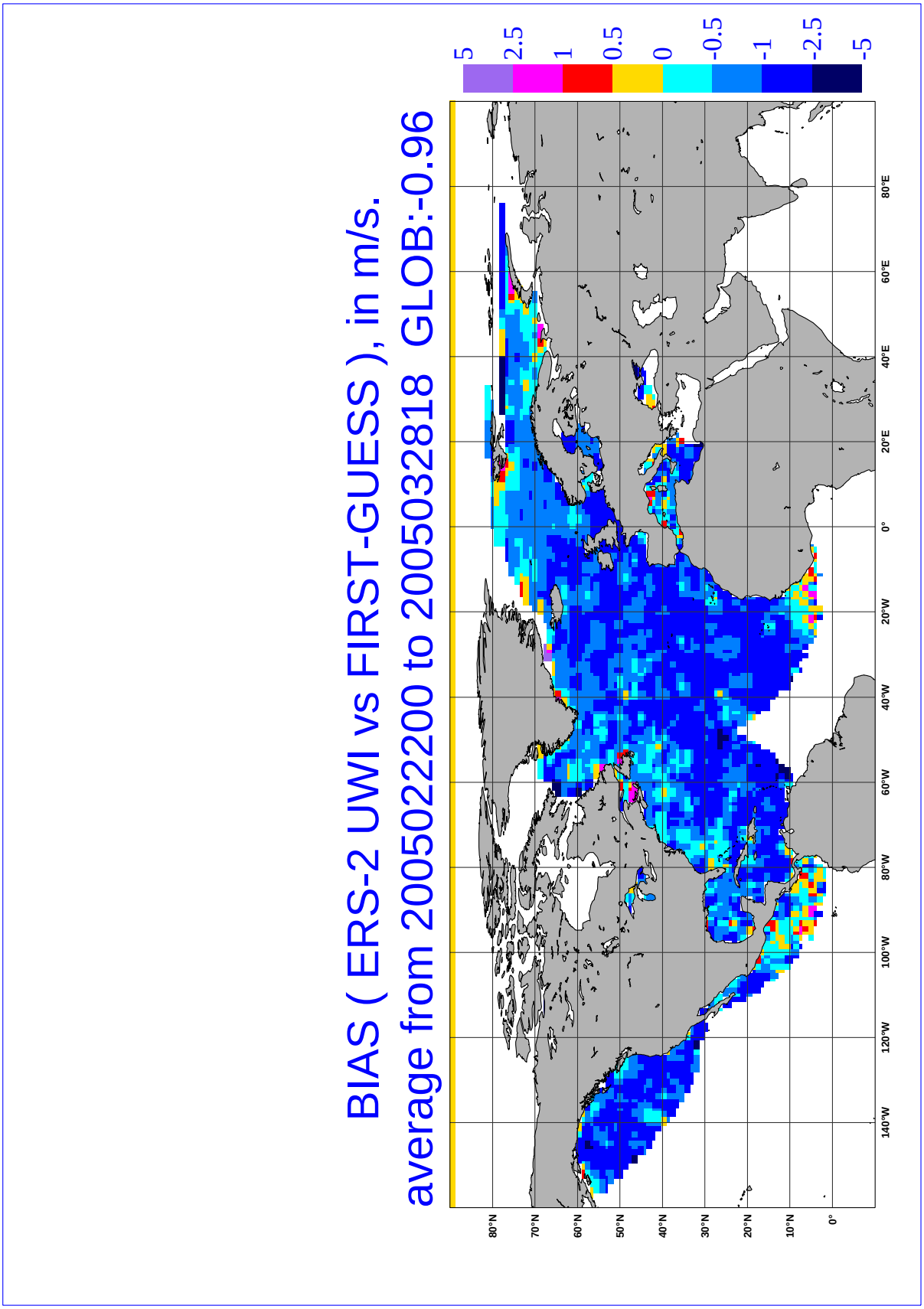
BIAS (ERS-2 UWI vs FIRST-GUESS), in m/s.
average from 2005022200 to 2005032818 GLOB:-0.96
5
2.5
1
0.5
0
-0.5
-1
-2.5
-5
80°N
70°N
60°N
50°N
40°N
30°N
20°N
10°N
0°
80°E
60°E
40°E
20°E
0°
20°W
40°W
60°W
80°W
100°W
120°W
140°W

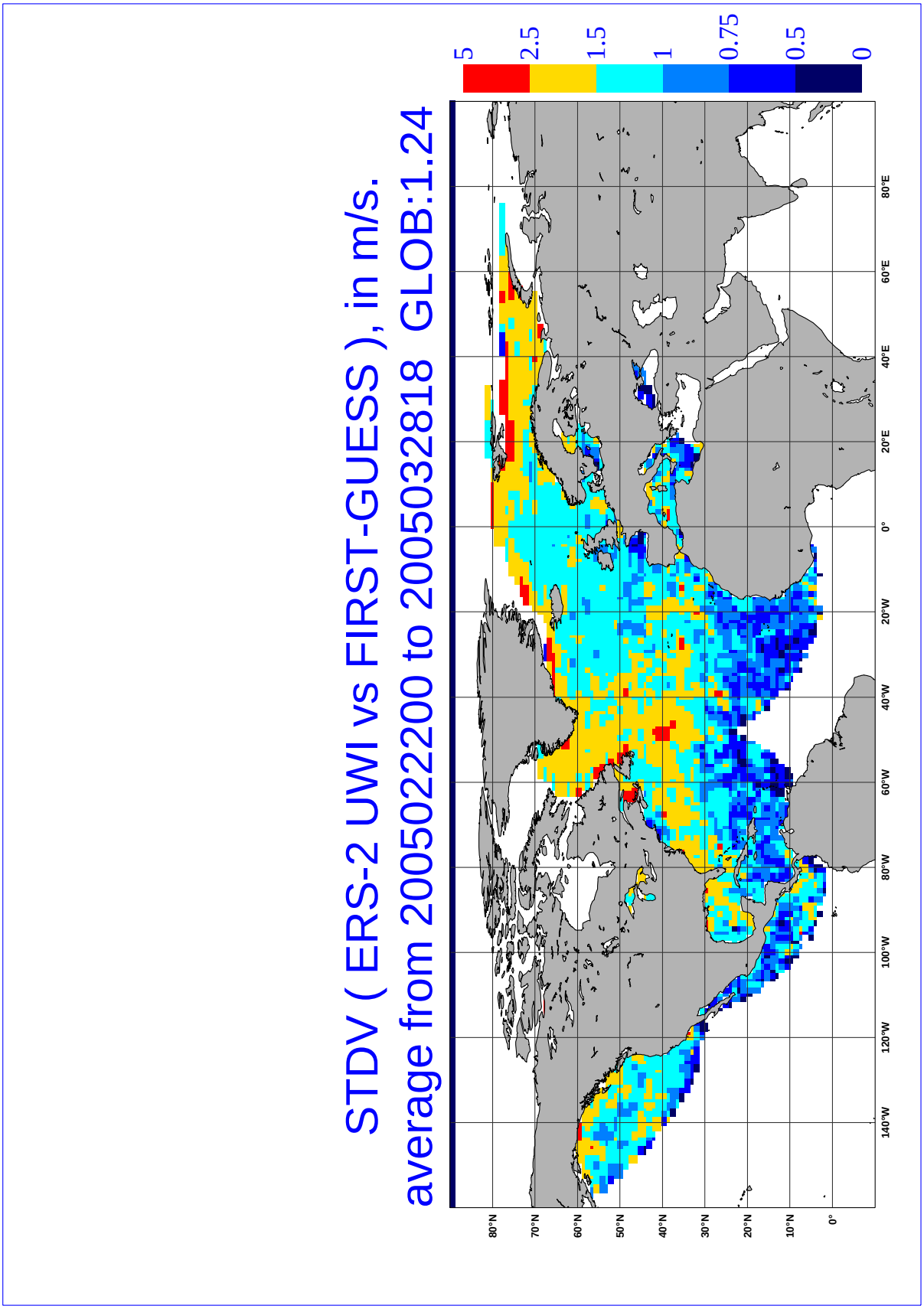

FIGURE 13 The same as Figure 12, but now for the relative bias (top panel) and standard deviation (lower panel) with ECMWF first-guess winds.

4.3.1 Distance to cone history

The distance to the cone history is shown in Figure 14. Curves are based on data that passed all QC, including the test on the Kp -yaw flag, however subject to the land and sea-ice check at ECMWF (see cyclic report 88 for details).

Like for cycle 102, time series are (due to lack of statistics) very noisy, especially for the first nodes. Most spikes were found to be the result of low data volumes.
Compared to cycle 102, the average level was lower (from 1.18 to 1.14), and is now about 5% higher than for nominal data (see top panel Figure 11).

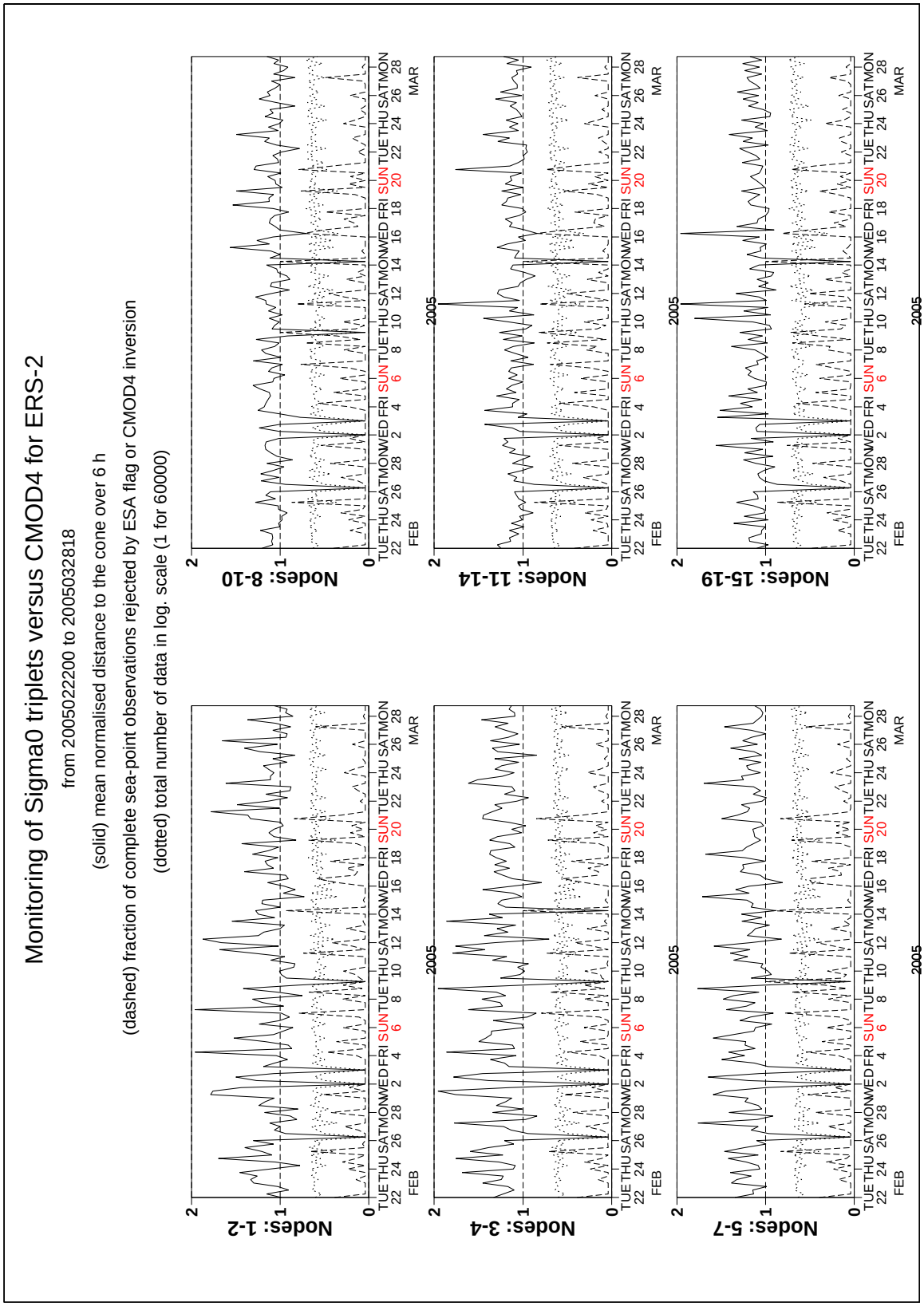

FIGURE 14 Mean normalized distance to the cone computed every 6 hours for nodes 1-2, 3-4, 5-7, 8-10, 11-14 and 15-19 (solid curve close to 1 when no instrumental problems are present). The dotted curve shows the number of incoming triplets in logarithmic scale (1 corresponds to 60,000 triplets) and the dashed one indicates the fraction of complete (based on the land and sea-ice mask at ECMWF) sea-located triplets rejected by ESA flags, or by the wind inversion algorithm (0: all data kept, 1: no data kept).

4.3.2 UWI minus First-Guess history

In Figure 15, the UWI minus ECMWF first-guess wind-speed history is plotted. The history plot shows several peaks, most of which are related to low data volumes. Similar results apply for the history of de-aliased CMOD4 winds versus FG (Figure 17).

Figure 19 displays the locations for which UWI winds were more than 8 m/s weaker (top panel) and more than 8 m/s stronger (lower panel) than FG winds. Like for cycle 101, the number of such collocations is low.

In the top panel of Figure 20 one case of much stronger UWI winds is illuminated in the Barentsz Sea on 28 February 2005. The patch of strong and probably incorrectly de-aliased UWI winds might well indicate the presence of sea-ice not present in the SSM/I derived ice map as used at ECMWF. During cycle 103 and previous cycles several of such cases can be identified in the lower panel of Figure 20 of the corresponding monitoring reports. The lower panel of Figure 20 displays a case of low UWI winds on 24 March 2005 near the Azores. A patch of turning UWI winds looks erratic.

Average bias levels and standard deviations of UWI winds relative to FG winds are displayed in Table 6.

Table 6 Wind speed and direction biases

	Cycle 102		**Cycle 103**	
	UWI	CMOD4	UWI	CMOD4
Speed STDV	1.56	1.55	1.55	1.54
Node 1-2	1.67	1.62	1.62	1.59
Node 3-4	1.57	1.55	1.56	1.55
Node 5-7	1.51	1.50	1.48	1.48
Node 8-10	1.50	1.50	1.48	1.48
Node 11-14	1.49	1.49	1.51	1.51
Node 15-19	1.51	1.51	1.55	1.55
Speed BIAS	-0.65	-0.63	-0.72	-0.70
Node 1-2	-1.27	-1.23	-1.23	-1.20
Node 3-4	-0.99	-0.92	-0.94	-0.89
Node 5-7	-0.70	-0.67	-0.74	-0.70
Node 8-10	-0.50	-0.50	-0.60	-0.59
Node 11-14	-0.42	-0.42	-0.57	-0.57
Node 15-19	-0.40	-0.41	-0.52	-0.53
Direction STDV	27.4	18.7	33.2	19.1
Direction BIAS	-3.1	-2.8	-2.7	-3.0

From this it is seen that the bias of both the UWI and CMOD4 product have become more negative, mainly at higher nodes. The average bias level is still less negative to that for nominal data in 2000 (UWI: -0.72 m/s now, was -0.79 m/s for cycle 59). The evolution of the bias from cycles 92 to 103 is displayed in the top panel of Figure 25. The red curve is the 15-day moving average for the at ECMWF inverted ERS-2 winds; i.e., CMOD5 since 9 March 2004. Blue vertical dashed lines indicate ECMWF model changes. This plot shows that the up-going line since end July 2004 has stabilized since November 2004. For QuikSCAT, the

positive trend in the globally averaged bias of (at ECMWF inverted and bias-corrected) QuikSCAT winds (middle panel) did continue until end 2004. Although averaged over all nodes the standard deviation of UWI winds compared to cycle 102 has hardly changed (1.55 m/s, was 1.56 m/s), it was reduced for lower incidence angles and did become larger at high range. For cycle 103 the (UWI - FG) direction standard deviations were ranging between 15 and 40 degrees, with the exception for the period between 6 and 9 March 2005. This anomalous behavior was not observed for the corresponding statistics for at ECMWF de-aliased CMOD4 winds, and therefore indicates a temporarily difficulty in the ESACA de-aliasing algorithm. As a result, the average performance for UWI wind direction degraded from 27.4 to 33.2 degrees, while the STDV for de-aliased winds was more stable (from 18.7 to 19.1degrees). Bias levels had hardly changed (around -3 degrees).

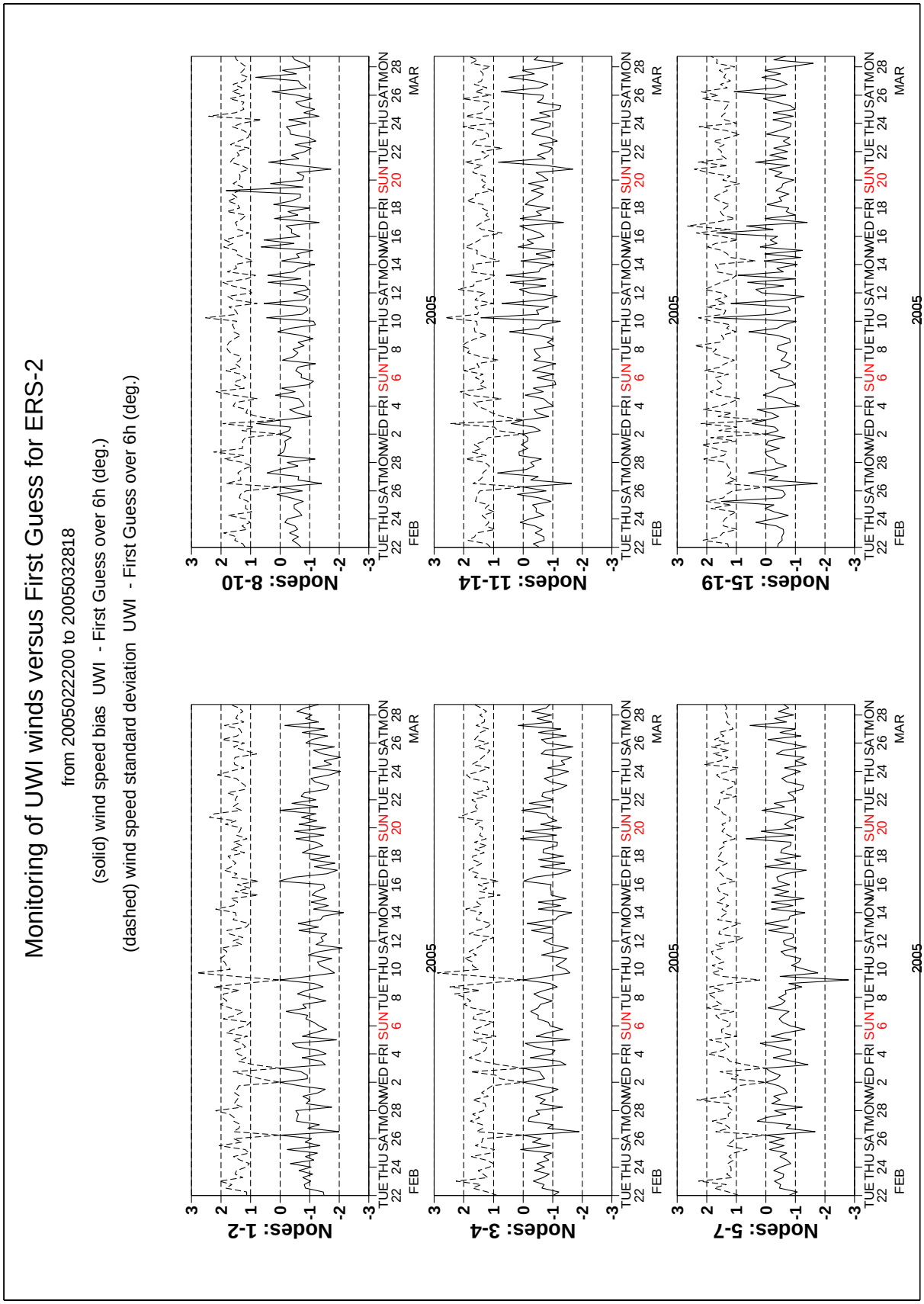

FIGURE 15 Mean (solid line) and standard deviation (dashed line) of the wind speed difference UWI - first guess for the data retained by the quality control.

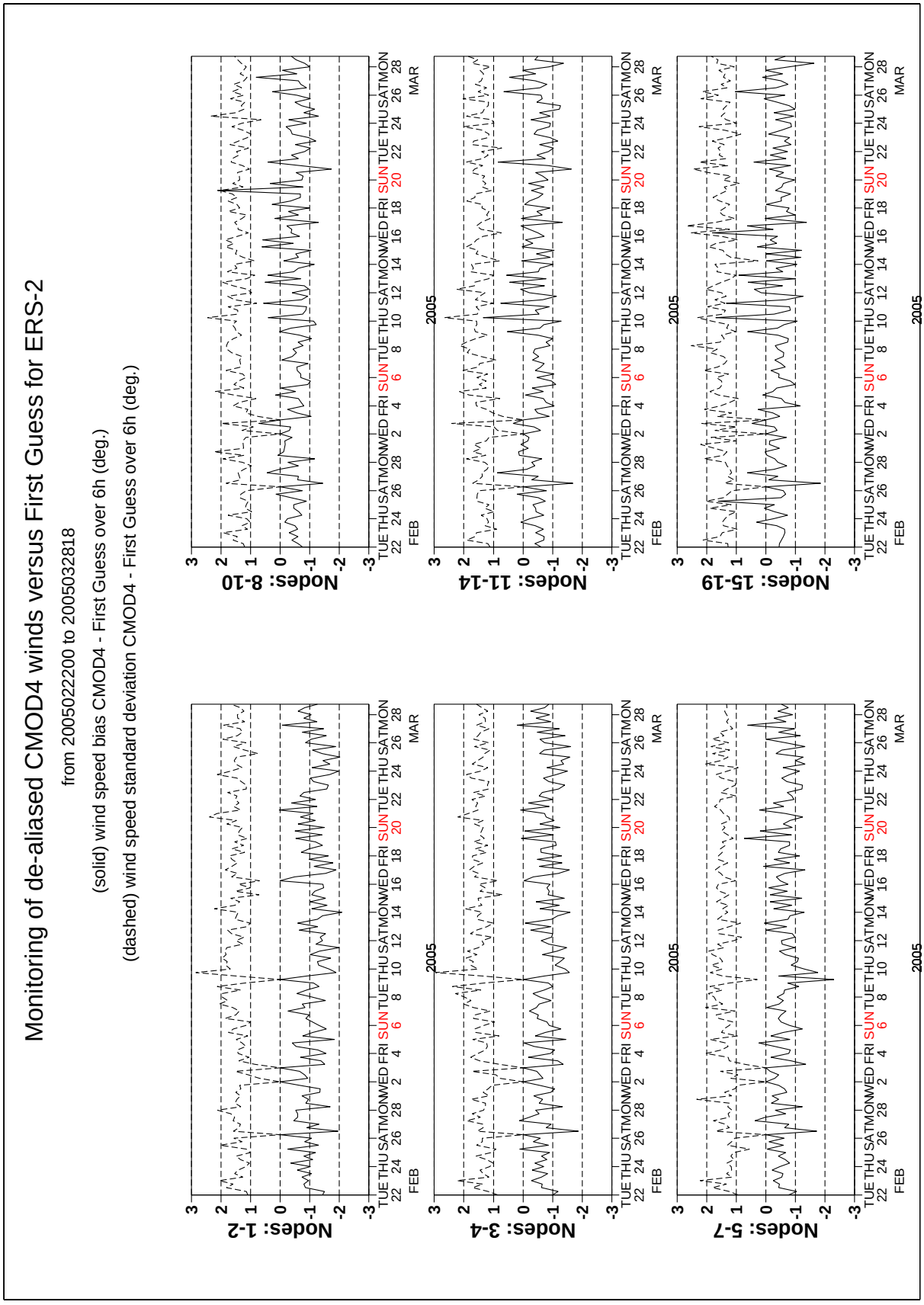

FIGURE 16 Same as Fig. 15, but for the de-aliased CMOD4 data.

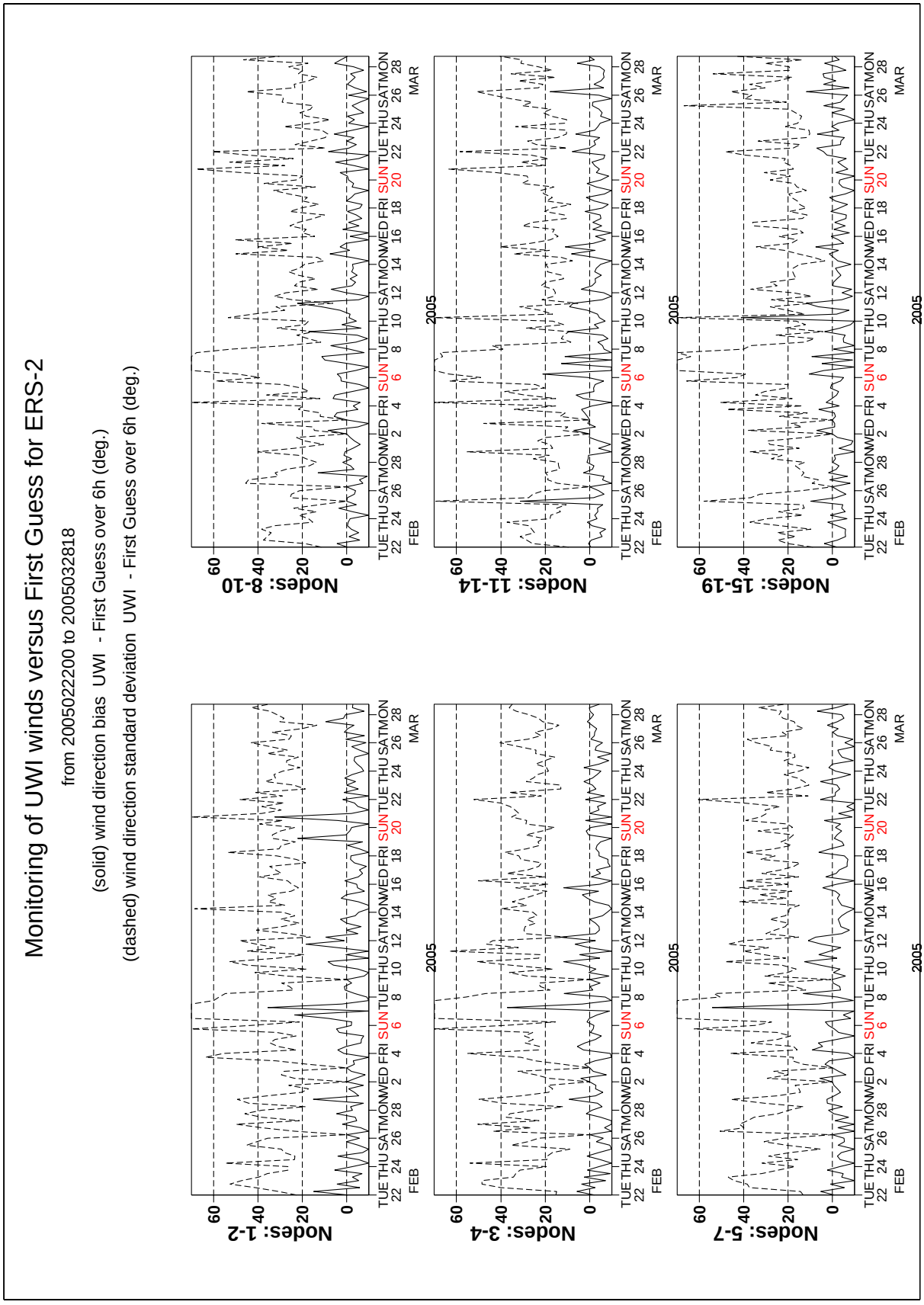

FIGURE 17 Same as Fig. 15, but for the wind direction difference. Statistics are computed only for wind speeds higher than 4 m/s.

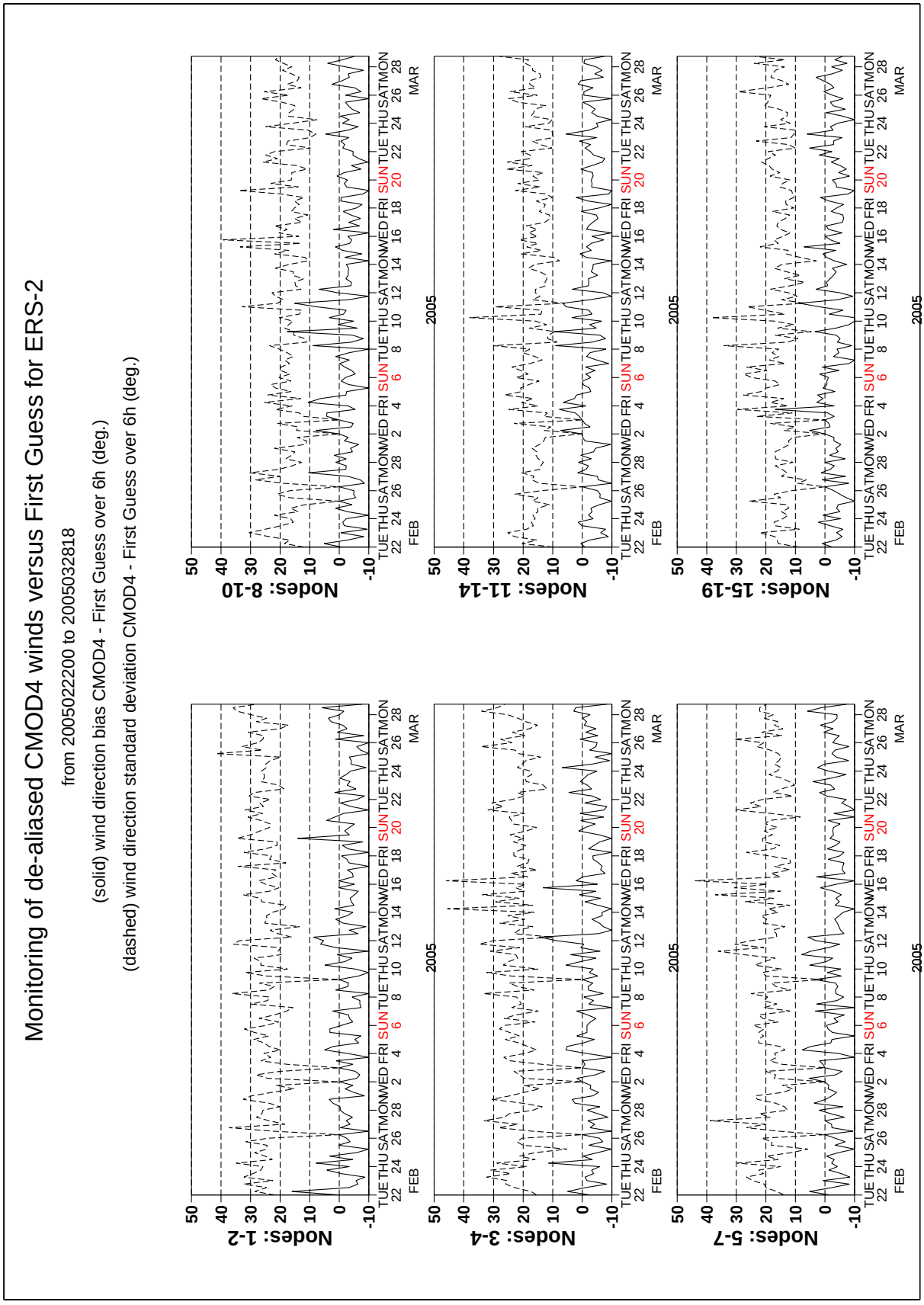

FIGURE 18 Same as Fig. 17, but for the de-aliased CMOD4 data.

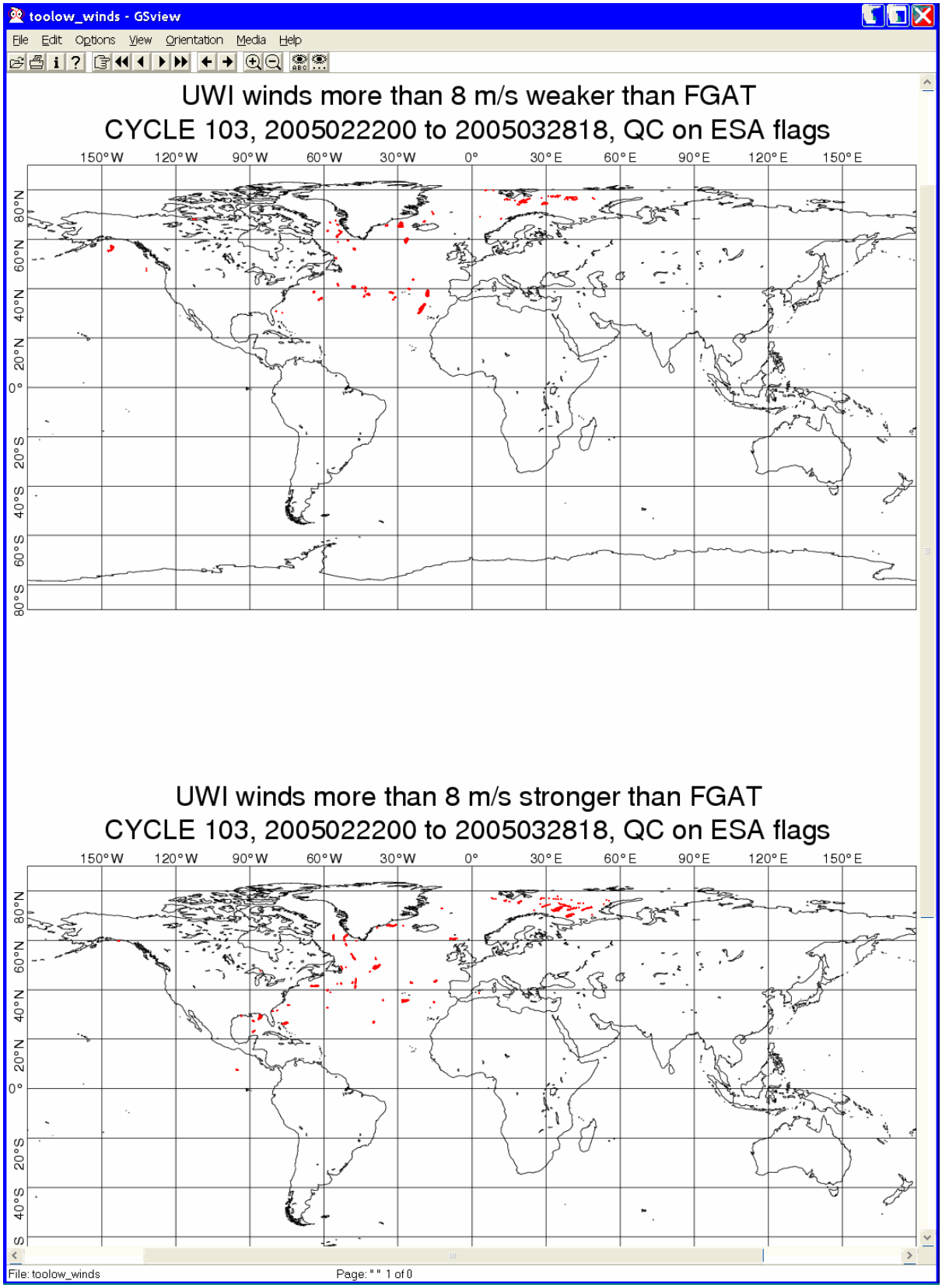

FIGURE 19 Locations of data during cycle 103 for which UWI winds are more than 8 m/s weaker (top panel) respectively stronger (lower panel) than FGAT, and on which QC on UWI flags and the ECMWF land/sea-ice mask was applied.

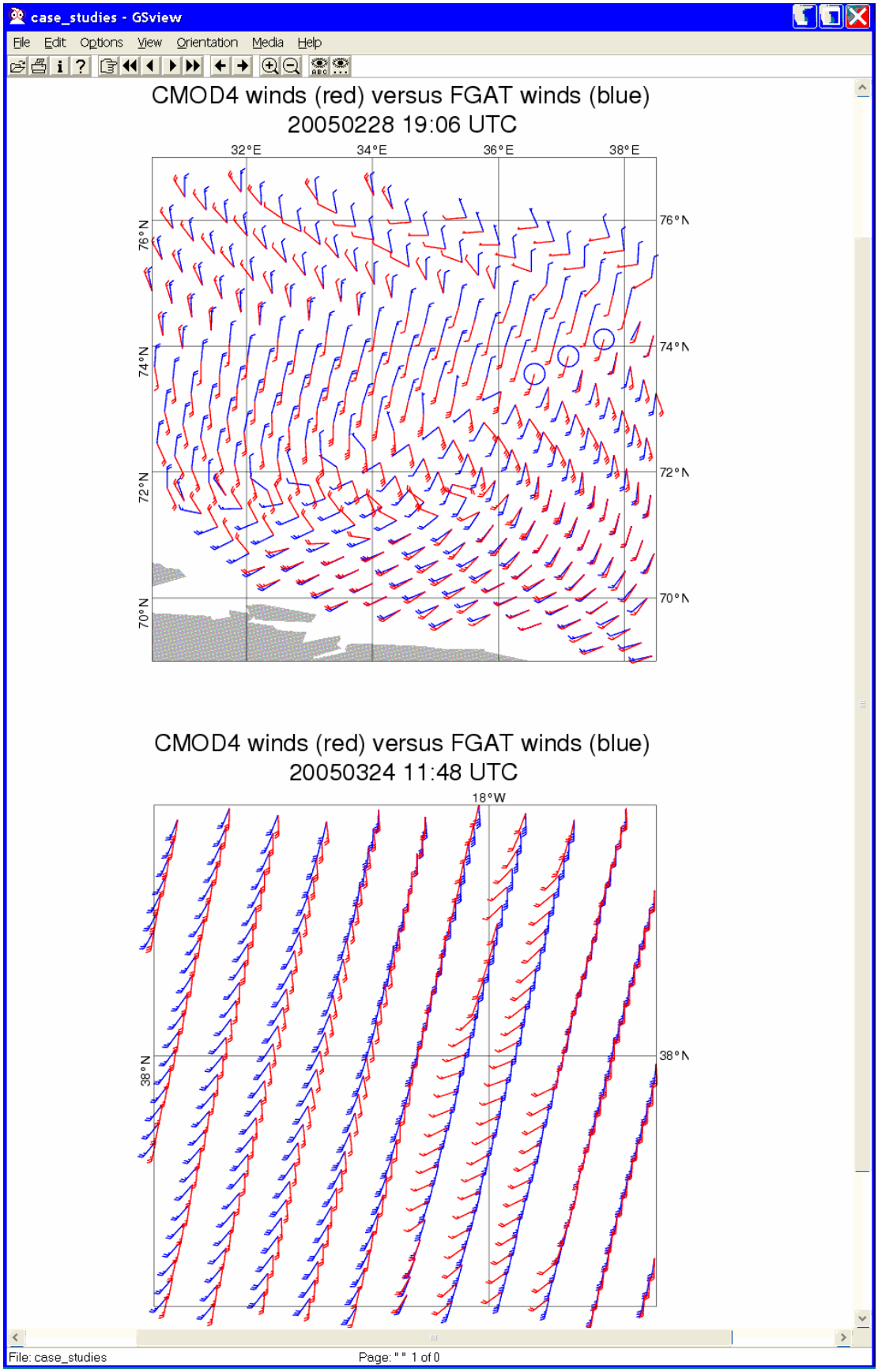

FIGURE 20 Comparison between UWI (red) and ECMWF FG (blue) winds for a case in the Barentsz Sea on 28 February 2005 (top panel) and near the Azores on 24 March 2005 (lower panel)

4.3.3 Scatter plots

Scatter plots of FG winds versus ERS-2 winds are displayed in Figures 21 to 24. Values of standard deviations and biases are slightly different from those displayed in Table 6. Reason for this is that, for plotting purposes, the in 0.5 m/s resolution ERS-2 winds have been slightly perturbed (increases scatter with 0.02 m/s), and that zero wind-speed ERS-2 winds have been excluded (decreases scatter with about 0.05 m/s).

The scatter plot of UWI wind speed versus FG (Figure 21) is very similar to that for (at ECMWF inverted) de-aliased CMOD4 winds (Figure 23). It confirms that the ESACA inversion scheme is working properly. The reduced standard deviation compared to cycle 101 (1.58 m/s, was 1.71 m/s), originates from a less intense wind climate.

Winds derived on the basis of CMOD5 are displayed in Figure 24. The relative standard deviation is lower than for CMOD4 winds (1.53 m/s versus 1.57 m/s).

Compared to ECMWF FG, CMOD5 winds are -0.18 m/s slower. For strong winds, a large negative bias as observed before cycle 102 was less present.

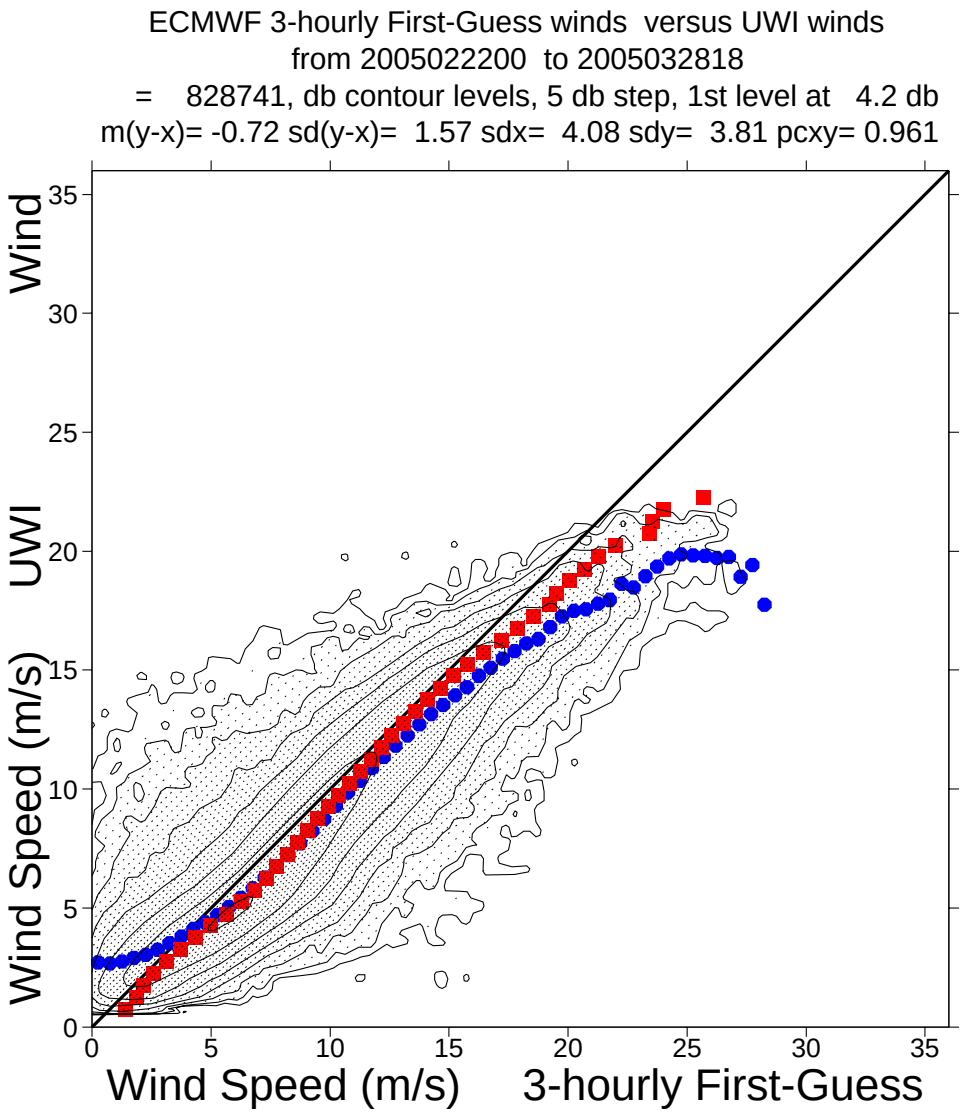

FIGURE 21 Two-dimensional histogram of first guess and UWI wind speeds, for the data kept by the UWI flags, and QC based on the ECMWF ice and land and sea-ice mask. Circles denote the mean values in the y-direction, and squares those in the x-direction.

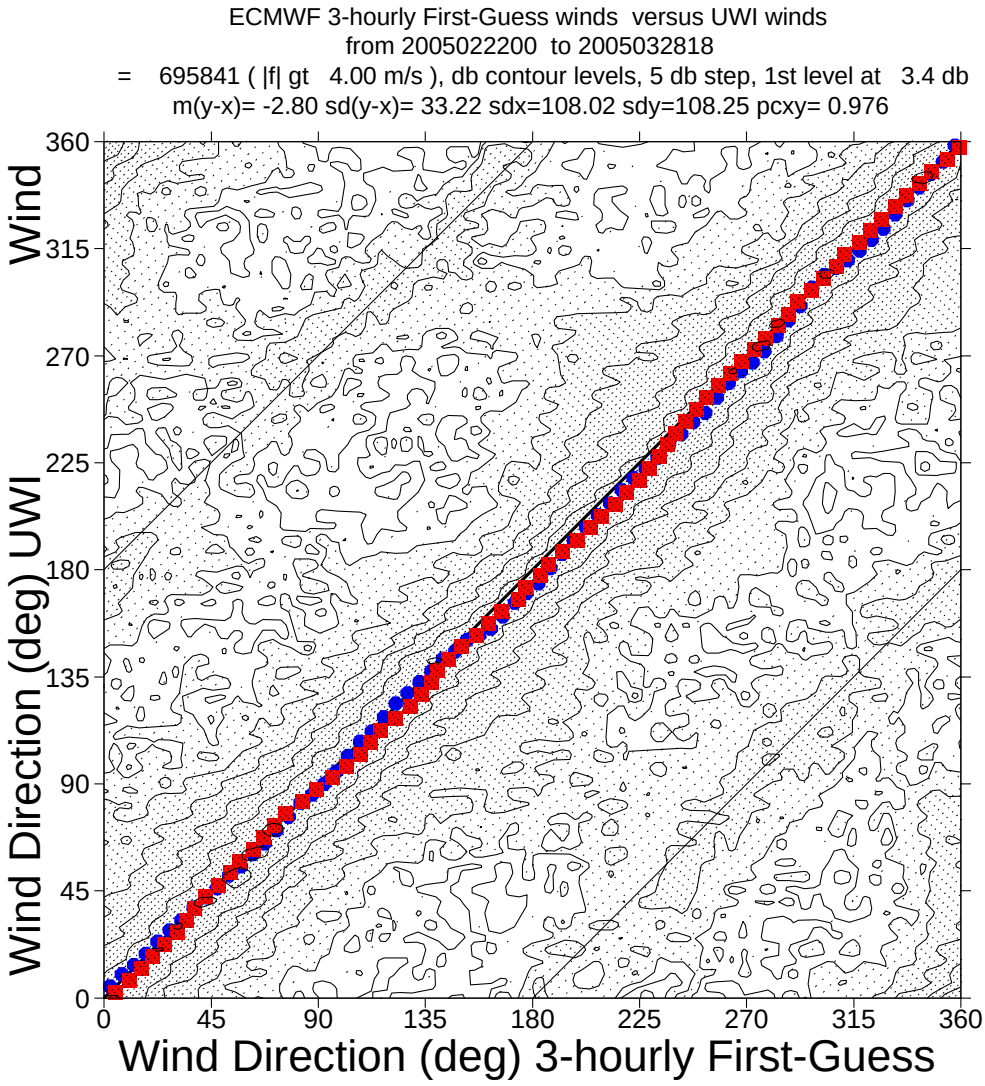

FIGURE 22 Same as Fig. 21, but for wind direction. Only wind speeds higher than 4m/s are taken into account.

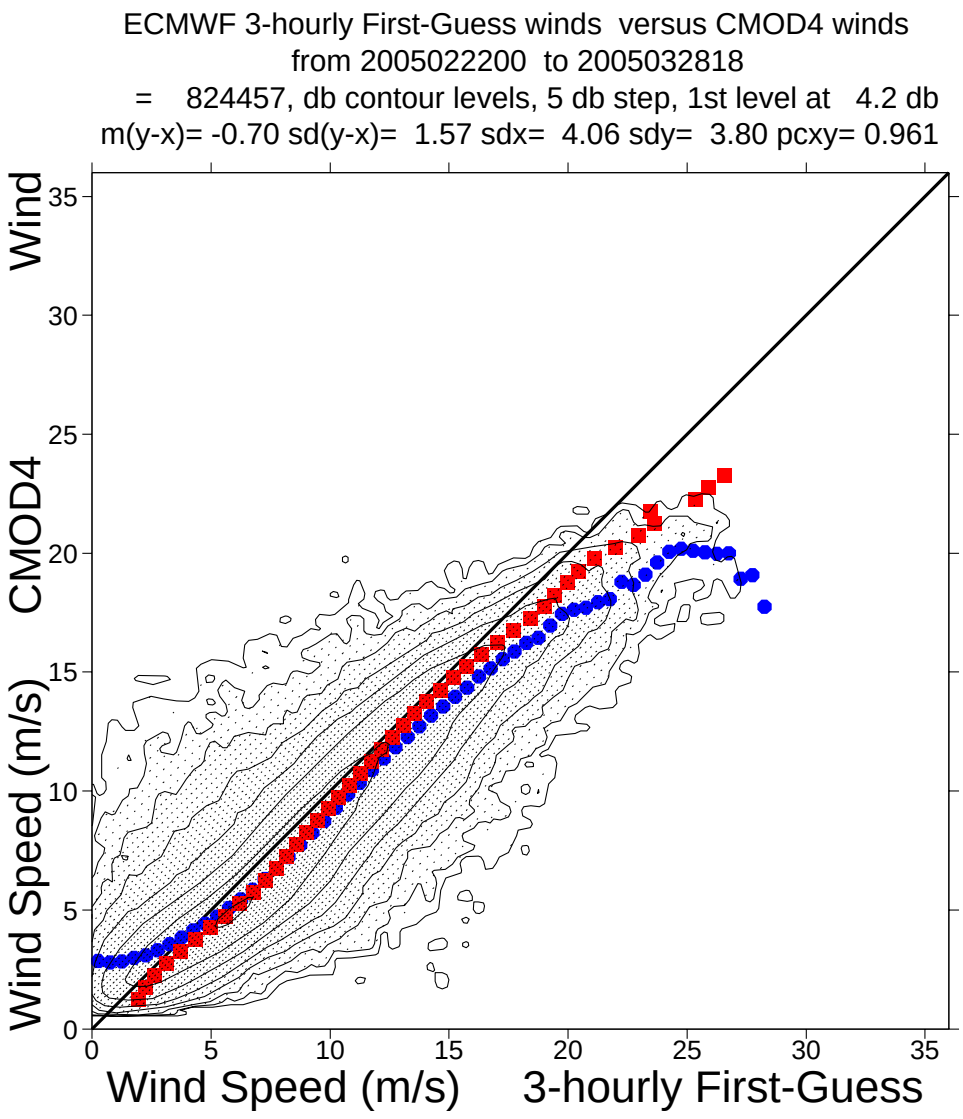

FIGURE 23 Same as Fig. 21, but for de-aliased CMOD4 winds.

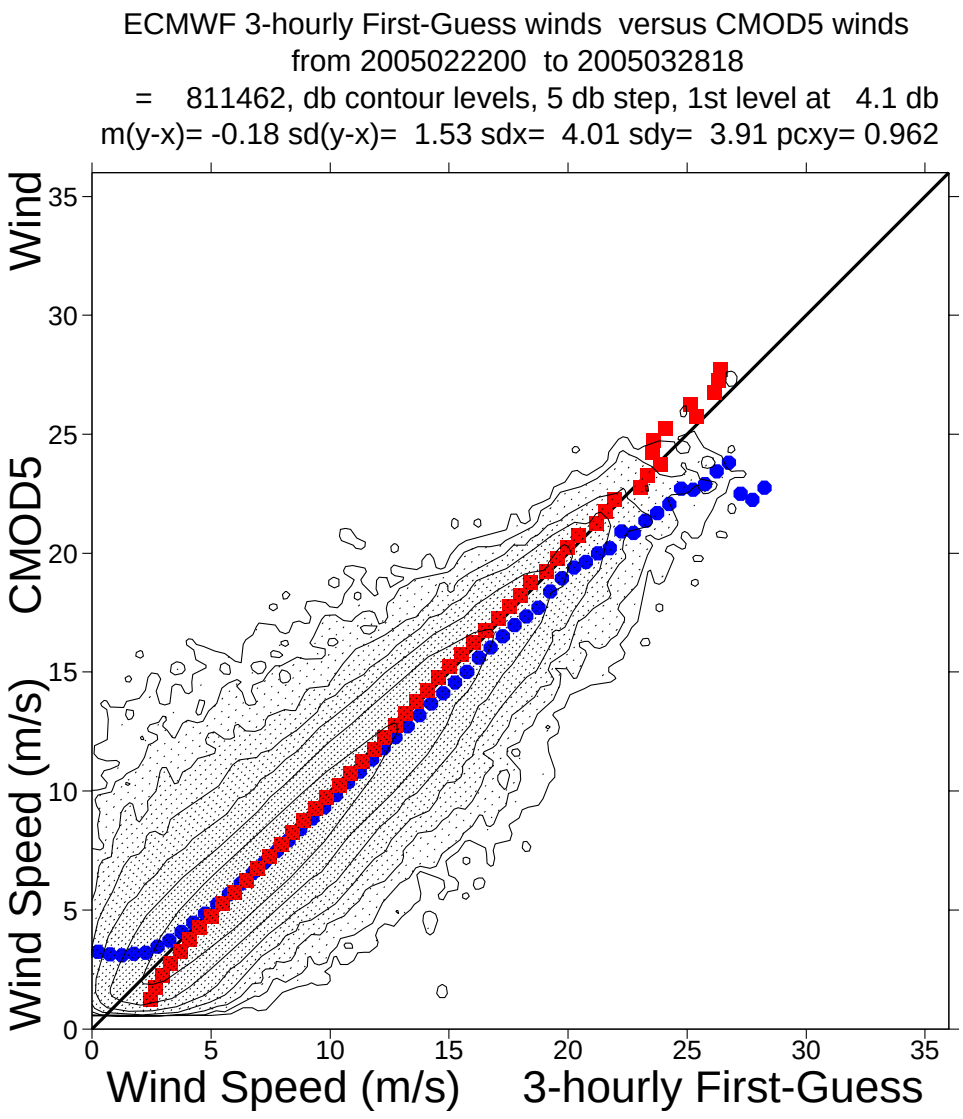

FIGURE 24 Same as Fig. 21, but for de-aliased CMOD5 winds.

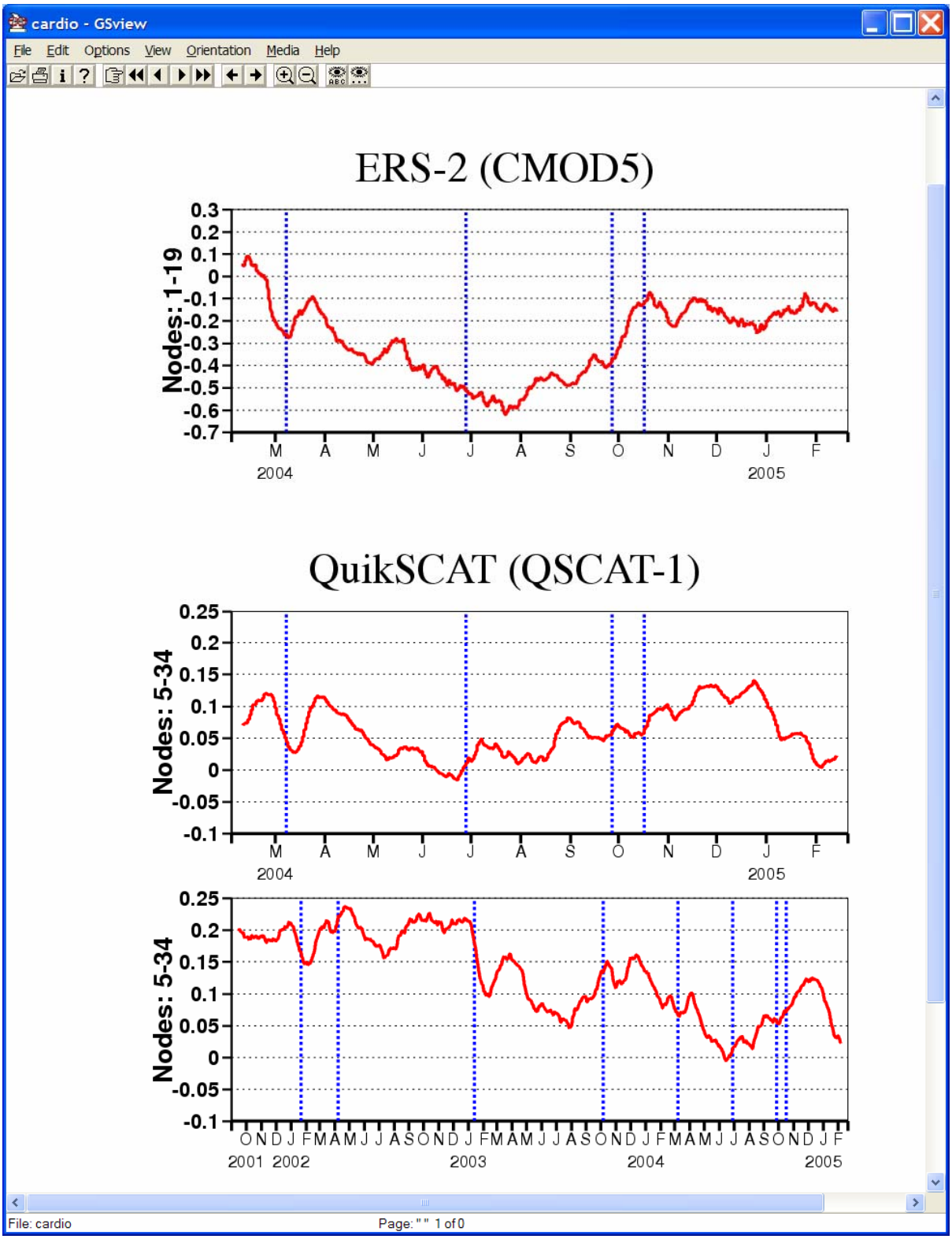

FIGURE 25 Bias relative to FG winds of the wind speed of ERS-2 winds (based on bias-corrected CMOD4 before 9 March 2004, and on CMOD5 afterwards) for nodes 1-19 (top panel) respectively of 50-km QuikSCAT (based on the QSCAT-1 model function) for nodes 5-34 (i.e., inner-beam zone; middle and lower panels)versus ECMWF first guess for the period of cycle 92 to 102.Curves represent centered 15-day running means for the top and middle panel, and a 30-day running mean for the lower panel. Vertical dashed blue lines mark ECMWF model changes

5 Yaw error angle estimation

The yaw error angle estimation is computed on-ground by the ESACA processors. The full set of results of the yaw processing is stored in an internal ESA product named HEY (Helpful ESA Yaw) disseminated from the ground station to ESRIN. The estimation of the yaw error angle is based on the Doppler shift measured on the received echo. That estimation can be done with a good accuracy only for small yaw error angle (in the range between +/-4 deg.). Above that range, due to high Doppler frequency shift the signal spectrum is outside the receiver bandwidth and the yaw estimation is strong degraded. Details regarding the yaw processing can be found on the following document (chapter 9): http://earth.esa.int/pcs/ers/scatt/articles/soamain-030521.pdf .

The yaw error angle estimation aims to compute the correct acquisition geometry for the three Scatterometer antenna throughout the entire orbit. The Yaw error angle information is used in the radar equation to derive the calibrated backscattering (sigma nought) from the Earth surface and to select the echo samples associated to one node. In ESACA the definition of the node position is as the one adopted in the old processor (for details see:.http://earth.esa.int/pcs/ers/scatt/articles/scatt_work98_processing.pdf). In such way the distance between the nodes (both along and across track) is kept constant (25 Km) and what is changing in function of the yaw error angle is the number of echo samples that contributes to the node calculation and the incidence angle of the measurement. This because the three Scatterometer antennae could see the node with a different geometry due to an arbitrary variation of the yaw angle along track. The number of samples that actually contributes to a node and the yaw flag can be retrieved from the UWI Data Set Record (DSR) product. For that reason the definition of few fields in the UWI product has been updated. For details see the Scatterometer cyclic report - cycle 90 -. The Figure 26 (since beginning of HEY dissemination) and Figure 27 (cycle) show for each orbit the average Doppler frequency shift (first 3 plots Fore Mid and Aft antenna), the minimum, maximum and mean yaw (fourth plot), the yaw standard deviation (fifth plot) and the percentage of source packets acquired with a yaw error angle outside the range +/- 2 degrees (sixth plot).
On average the yaw evolution is within the specification for the ESACA processor to assure calibrated data. The evolving yaw bias occurred in June 2004 has been reported to the flight segment and corrective actions have been put in place to compensate for.

The result of the yaw monitoring for cycle 103 is a yaw error angle within the expected nominal range (+/- 2 degrees) with an average level around 0 deg. for most of the orbit. Since mid March 2005 there was an improvement in the yaw performances (see the yaw standard deviation and yaw pcd plots in Figure 27). This is mainly due to the geometry of the Earths orbit that decreases the negative impact of the Sun within the field of view of the Earth sensor at the Eclipse to Sunlight transition (see previous report for details).

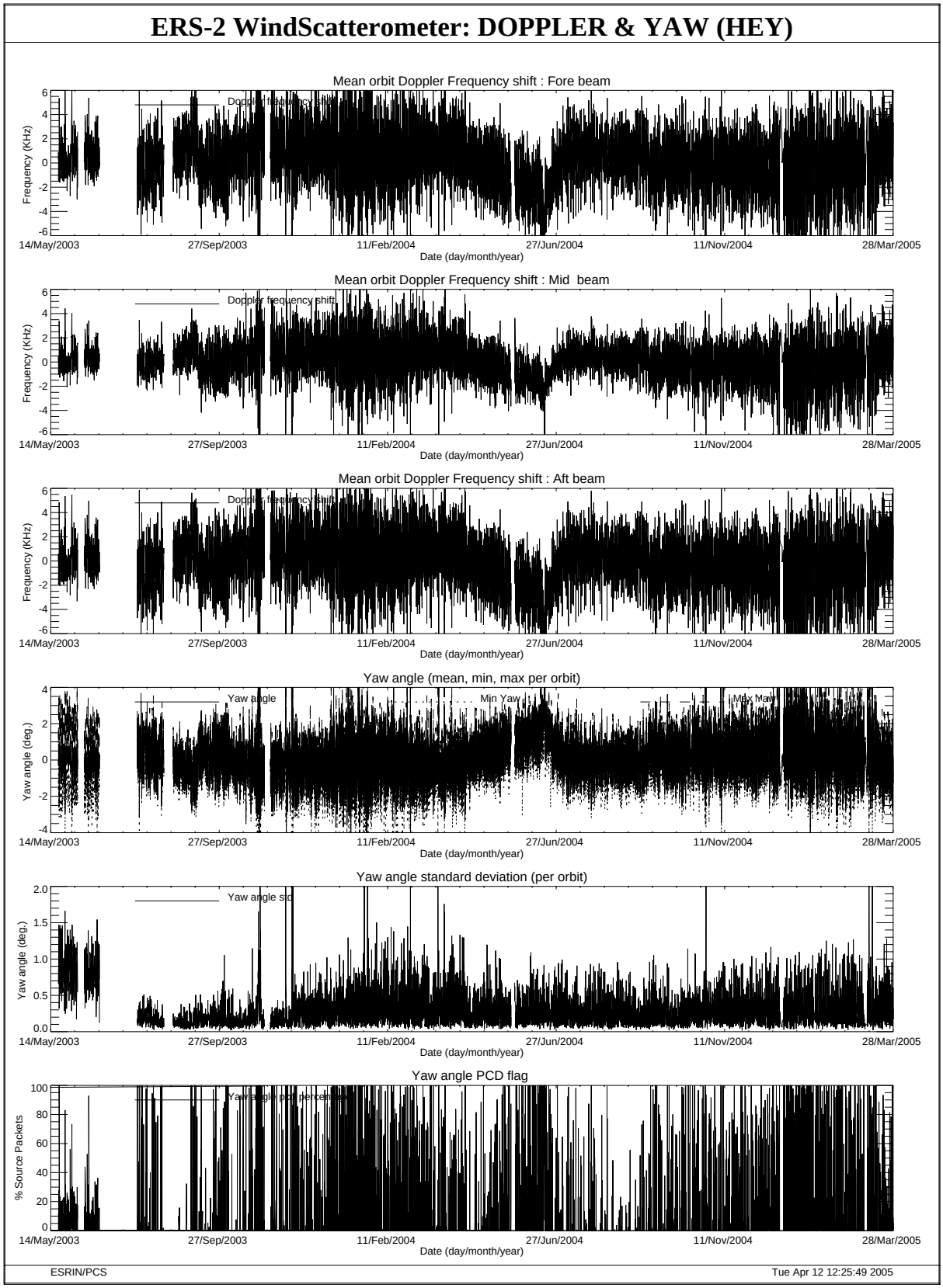

FIGURE 26 Doppler frequency shift and Yaw error angle evolution since August 2003.

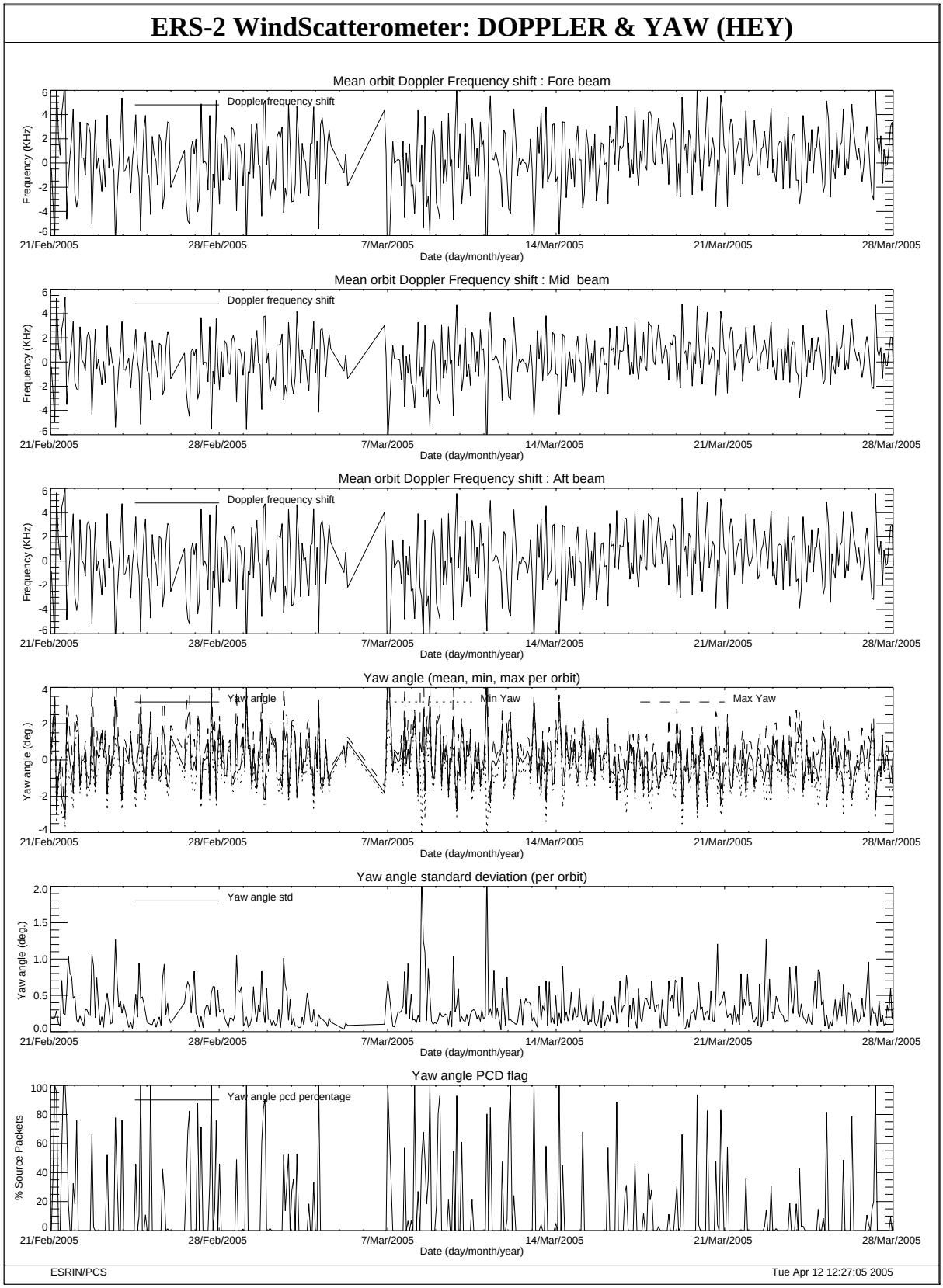

FIGURE 27 Doppler frequency shift and Yaw error angle evolution cycle 103.